THE UNIVERSITY OF ALBERTA

STIFFNESS OF CLAMPED JOINTS

by

Ⓒ DALLAS D. NELSON, B.Sc. (Alberta)

A THESIS
SUBMITTED TO THE FACULTY OF GRADUATE STUDIES
IN PARTIAL FULFILMENT OF THE REQUIREMENTS FOR THE DEGREE
OF MASTER OF SCIENCE

DEPARTMENT OF MECHANICAL ENGINEERING

EDMONTON, ALBERTA
SPRING, 1969

[illegible]

[illegible]

[illegible]

[illegible] ©

[illegible]
[illegible]
[illegible]
[illegible]

[illegible]

[illegible]
[illegible]

UNIVERSITY OF ALBERTA

FACULTY OF GRADUATE STUDIES

The undersigned certify that they have read, and recommend to the Faculty of Graduate Studies for acceptance, a thesis entitled "STIFFNESS OF CLAMPED JOINTS" submitted by DALLAS D. NELSON in partial fulfilment of the requirements for the degree of Master of Science.

ABSTRACT

Experiments were conducted to determine the effects of surface texture and normal load on the stiffness of joints formed by two machined surfaces. The experiments involved deformation measurements and examination of the contact surfaces of joints subjected to normal loads. The elastic stiffness of a joint was found to be affected by the loading history and surface profile measurements indicated that the topography of the joint surfaces changed with normal load. Discrepancies arose between the experimental load deformation results and empirical relations proposed by Connolly and Thornley. It is suggested that the method used to assess surface texture in these empirical relations is inadequate for predicting the stiffness of an individual joint.

ACKNOWLEDGEMENTS

The author wishes to express his gratitude to the following who contributed to this thesis:

- Dr. D.G. Bellow for his supervision, guidance, and encouragement in preparing this thesis.
- Members of the Mechanical Engineering Department shop for preparing experimental apparatus.
- Miss L. Fiveland for her excellent typing of the thesis.
- The University of Alberta and the National Research Council for providing funds that made this thesis possible.

TABLE OF CONTENTS

CHAPTER PAGE

I. INTRODUCTION 1

1.1 Introduction to the Problem 1

1.2 Description of Surface Texture 2

1.3 Historical Review 4

1.4 Aims of the Thesis 8

II. EXPERIMENTAL PROCEDURE AND APPARATUS 9

2.1 Introduction 9

2.2 Procedures Common to Tests I, II, and III 10

2.2-1 Nominal Surface Pressure 10

2.2-2 Surface Displacement 10

2.2-3 Surface Texture Measurements 12

2.2-4 Bearing Area 13

2.3 Test I 13

2.4 Tests II and III 14

III. RESULTS 23

3.1 Strain Gauge Results 23

3.1-1 Differences in Strain Gauge Results Between the Two Specimens in Test I 23

3.1-2 Differences in Strain Gauge Results for Test II 23

3.1-3 Check on the Strain Gradient 24

3.1-4 The Effect of Strain Obtained from Strain Gauges on the Extensometer Deflection 25

CHAPTER PAGE

3.1-5 The Effect of Strain on the Recoverable Surface Displacement 26
3.2 General Shape of the Loading Envelopes 27
3.3 Total and Permanent Surface Displacement Results . . 28
3.4 Permanent Change in Surface Profile with Load 30
3.5 Bearing Area Results 32
3.6 Recoverable Surface Displacement Results 33
3.7 Summary of Results 36
IV. CONCLUSIONS AND RECOMMENDATIONS 75
Conclusions 75
Recommendations 75
REFERENCES 77
APPENDIX A Geometry of a surface produced by a single point cutting tool 78
APPENDIX B Relation for total joint deflection reported by Connolly and Thornley 82
APPENDIX C Model for surface displacement 84

LIST OF TABLES

TABLE PAGE

2-1 Joint Specimens Test I 14

2-2 Machining Conditions for Turned Surfaces 16

3-1 Difference in Strain Gauge Values after a Maximum NSP of 20,000 psi, Test I 38

3-2 Individual Strain Gauge Results for Test II 39

3-3 Permanent Change in Profile after an NSP of 4,000 psi, Test II 40

3-4 Average Strain Gauge Results used for Recoverable Surface Displacement Curves, Test I 40

3-5 Average Strain Gauge Results used for Recoverable Surface Displacement Curves, Test II 41

3-6 Average Strain Gauge Results used for Recoverable Surface Displacement Curves, Test III 42

3-7 CLA and m Values for the Rough Specimens in Tests I, II, and III 43

LIST OF FIGURES

FIGURE PAGE

1-1 Definition of CLA 3

1-2 Method of Obtaining the Bearing Area 5

1-3 General Shape of Loading Envelope 6

2-1 Arrangement of Extensometer and Strain Gauges 19

2-2 Datum for Surface Measuring Instrument 20

2-3 Joint Specimen, Tests II and III 21

2-4 Surface Profile Measurement 22

2-5 Loading Arrangement 22

3-1 Strain Gauge Results for Test I after 20 ksi Nominal Surface Pressure 44

3-2 Strain Gauge Results for Test II after 20 ksi Nominal Surface Pressure 45

3-3 Strain Gauge Results for Test III after 20 ksi Nominal Surface Pressure 46

3-4 Strain Gradient Test II 47

3-5 Strain Gauge Deflection ($\varepsilon\ell$) as Percent of Extensometer Measurement, Test I 48

3-6 Strain Gauge Deflection ($\varepsilon\ell$) as Percent of Extensometer Measurement, Test II 49

3-7 Strain Gauge Deflection ($\varepsilon\ell$) as Percent of Extensometer Measurement, Test III 50

3-8 Average Strain Gauge Results after 20 ksi Nominal Surface Pressure 51

FIGURE PAGE

3-9 Recoverable Surface Displacement Based on Strain Gauge Results and Assumed Strain 52

3-10 Loading Envelope, Test I 53

3-11 Loading Envelope, Test II 54

3-12 Loading Envelope, Test III 55

3-13 Total Surface Displacement, Tests II and III 56

3-14 Permanent Surface Displacement, Tests II and III 57

3-15 Comparison of Total Displacement with Results Obtained by Connolly and Thornley for Test I 58

3-16 Comparison of Total Displacement with Results Obtained by Connolly and Thornley for Tests II and III 59

3-17 Surface Profiles of the Turned Specimen in Test II 60

3-18 Surface Profiles of the Ground Specimen in Test II 61

3-19 Surface Profiles of the Turned Specimen in Test III . . . 62

3-20 Surface Profiles of the Ground Specimen in Test III . . . 63

3-21 Comparison of Extensometer Measurements with Profile Measurements, Test II 64

3-22 Bearing Area for the Turned Specimen in Test II 65

3-23 Bearing Area Results 66

3-24 Recoverable Surface Displacement, Test I 67

3-25 Recoverable Surface Displacement, Test II 68

3-26 Recoverable Surface Displacement, Test II 69

3-27 Recoverable Surface Displacement, Test III 70

3-28 Recoverable Surface Displacement, Test III 71

FIGURE PAGE

3-29 Comparison of Recoverable Displacement with Results Obtained by Connolly and Thornley for Test I 72

3-30 Comparison of Recoverable Displacement with Results Obtained by Connolly and Thornley for Test II 73

3-31 Comparison of Recoverable Displacement with Results Obtained by Connolly and Thornley for Test III 74

A-1 Surface Profile 81

A-2 Cutting Tool 81

A-3 Coordinates for CLA value 81

A-4 Coordinates for Bearing Area 81

B-1 Functions z and K, Connolly and Thornley 83

C-1 Combination of Friction and Spring Elements 87

C-2 Load Deflection Curve for One Set of Elements 87

C-3 Distribution of Elements 87

C-4 Deflection of One Element 87

C-5 Loading Envelope 87

NOTATION

A	area
E	modulus of elasticity
P	nominal surface pressure (NSP)
x	surface displacement (x, y are also used as symbols for rectangular coordinates)
ℓ	gauge length
ε	strain
δ	extensometer deflection
F	feed rate
D	depth of cut
d	height of tool marks
R	tool radius
θ	angle
λ	joint deflection (Connolly and Thornley)
m	constant relating NSP and elastic joint deflection
z	function relating NSP and total joint deflection
L	cut-off length
CLA	center line average

Other symbols are defined when used.

CHAPTER I

INTRODUCTION

1.1 Introduction to the Problem

Machines are usually built of several component parts. This may be done to permit relative motion between the parts, fabrication, transportation or maintenance. The performance of a joint is partly dependent on its function within the machine and can involve several factors; stiffness, damping, resistance to sliding, and wear. However, in this study the assessment of joint performance will be based on stiffness alone.

Whenever separate machine elements are mechanically clamped together to form joints within a structure, the joints themselves will contribute to the deflection under load and can cause a significant reduction in the overall stiffness of the machine structure. The more rigid the machine the better the performance, the lower the amplitude of vibration, and the closer are the tolerances that can be maintained. Thus a knowledge of joint stiffness is important in design in the machine tool industry.

The reduction in stiffness due to a joint can be examined by comparing two metal components in mechanical contact with a single solid component of the same material and dimensions. If a compressive load is applied to the joined parts in a direction normal to the contact surfaces, deflection between gauge points on either side of the joint will be larger than the deflection over the corresponding gauge length

in an equivalent solid component under the same normal loading.

The stiffness of a joint may be affected by the surface texture, the nominal shape of the contact surfaces (i.e. spherical, flat, etc.), the presence of debris or lubricant on the contact surfaces, the loading conditions, and the choice of materials used in the joint. The surface texture has a primary influence on the deflection of a joint under static normal load. The scope of this study will be confined to the evaluation of the effects of surface texture on the stiffness of clamped, non-lubricated machine elements loaded in the direction normal to their nominally flat contact surfaces.

1.2 Description of Surface Texture

The surface texture of a joint is dependent on the method used to produce the surface. Surface texture has been defined [1]* as irregularities that tend to form a pattern on a surface, and has been divided into two parts; roughness and waviness. Roughness or primary texture describes the surface irregularities that are inherent in the method used to produce the surface. Tool geometry, cutting speeds and feed rates are some of the factors that would affect the roughness of a machined surface. Waviness or secondary texture is the component of surface texture on which the roughness is superimposed. It is due to a specific work piece and machine tool combination. Some factors that would produce waviness are; imperfect machine tool slide ways, vibrations,

---

* Numbers in brackets refer to references at the end of the thesis.

and machine tool stiffness.

Electronic instruments have been developed which use a diamond stylus that traverses across the surface, recording on electrical output proportional to the vertical movement of the stylus. These instruments record surface profiles or make a numerical assessment of surface texture. A common numerical assessment of surface texture is defined as follows: Refer the profile, y(x), shown in Figure 1-1 to a mean line, $y = 0$. The mean line is chosen so that the sum of the squares of the profile deviations from the mean line is a minimum over the cut-off length, L. The center line average is then defined as

$$\mathrm{CLA} = \frac{1}{L} \int_0^L |y| \, dx \, .$$

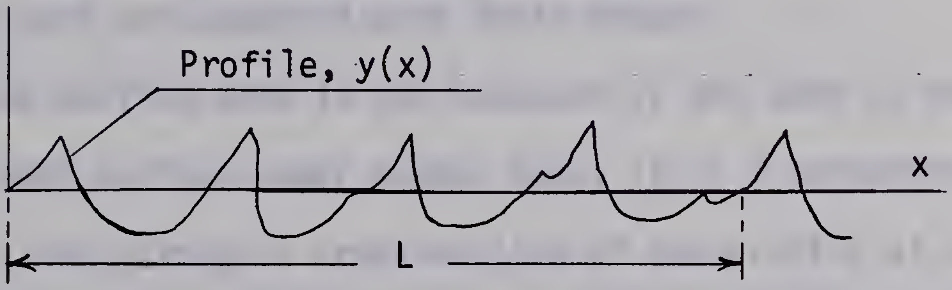

Figure 1-1 Definition of CLA

In this study surface texture will be assessed on the basis of its surface profile and CLA value.

1.3 Historical Review

In 1960, using an optical technique, Kragelsky and Demkin [2] observed the contact area of two solids. They pressed 5 m.m. diameter cylindrical specimens of lead, copper, and aluminum against the flat surface of a glass prism and obtained experimental curves of the contact area as a function of the normal compressive load. This technique yielded an experimental relationship between the load and the contact area, but did not represent deformation measurement in the direction of the load.

Kragelsky and Demkin also attempted to theoretically relate the load and surface deformation by using the concept of bearing area. They obtained a favourable comparison between theoretical and experimental contact areas as functions of load; however, experimental joint deflection results were not compared with their theory.

While the bearing area is not necessarily the same as the contact area for a joint surface under normal load, it is a convenient measure of the area taken through a cross-section of the profile of the surface. This was illustrated in 1933 by Abbott and Firestone [3] who defined bearing area as the fraction of the total length of a line, such as AB in Figure 1-2, that is enclosed by the surface profile. The bearing area can be obtained at several levels in the profile record and plotted as a function of distance in the direction normal to AB. The datum for the depth into the surface is chosen so that the bearing area is zero at the first point of contact as shown in Figure 1-2.

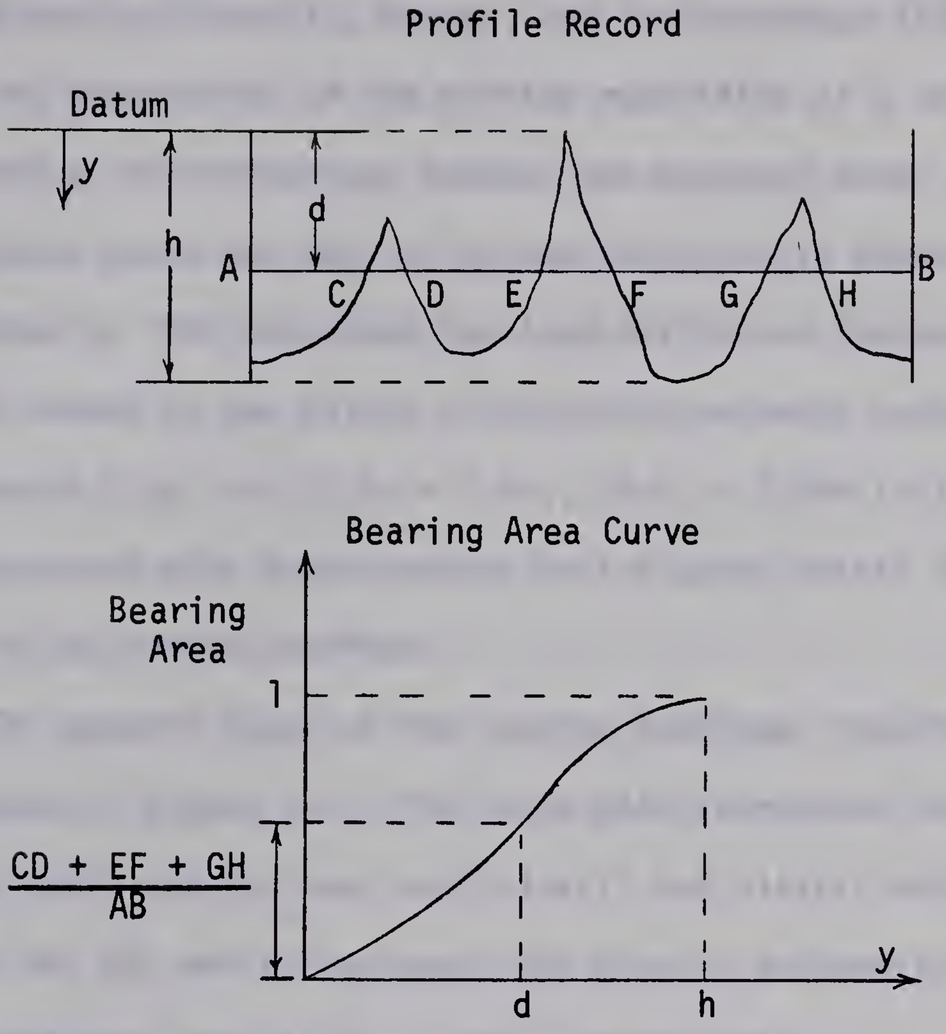

Profile Record

Bearing Area Curve

Figure 1-2 Method of Obtaining the Bearing Area

Deformation measurements across the contact surface of a joint were made by Ling [4] in 1958. His specimens were 0.5 in. diameter solid cylinders and the ends comprising the joint surfaces were ground (CLA of 4 to 20 μ-in.). The specimens were loaded normal to the joint surfaces and the change in distance between two gauge marks, initially 160 microns (6400 μ-in.) apart, on either side of the joint was measured with a microscope. Ling's load deflection results indicated that joint stiffness increased with an increase in normal load.

Thornley, Connolly, Barash, and Koenigsberger [5] have suggested that the deformation of the surface asperities of a joint interface can be found as the difference between the measured total deflection of the two joined parts and that of an equivalent solid piece. Their work published in 1965 described the load deflection characteristics of joints formed by two hollow cylindrical specimens having a cross sectional area of 2 sq. in. (I.D. = 1 in., O.D. = 1.884 in.). Deflections were measured with extensometers having gauge points 3/16 in. on either side of the contact surface.

The general shape of the loading envelopes reported in [5] is illustrated in Figure 1-3. The curve OACE represents the total deflection of the joint and includes both plastic and elastic deformation. The curves AB, CD, and EF represent the elastic deformation of the joint after maximum loads at A, C, and E respectively.

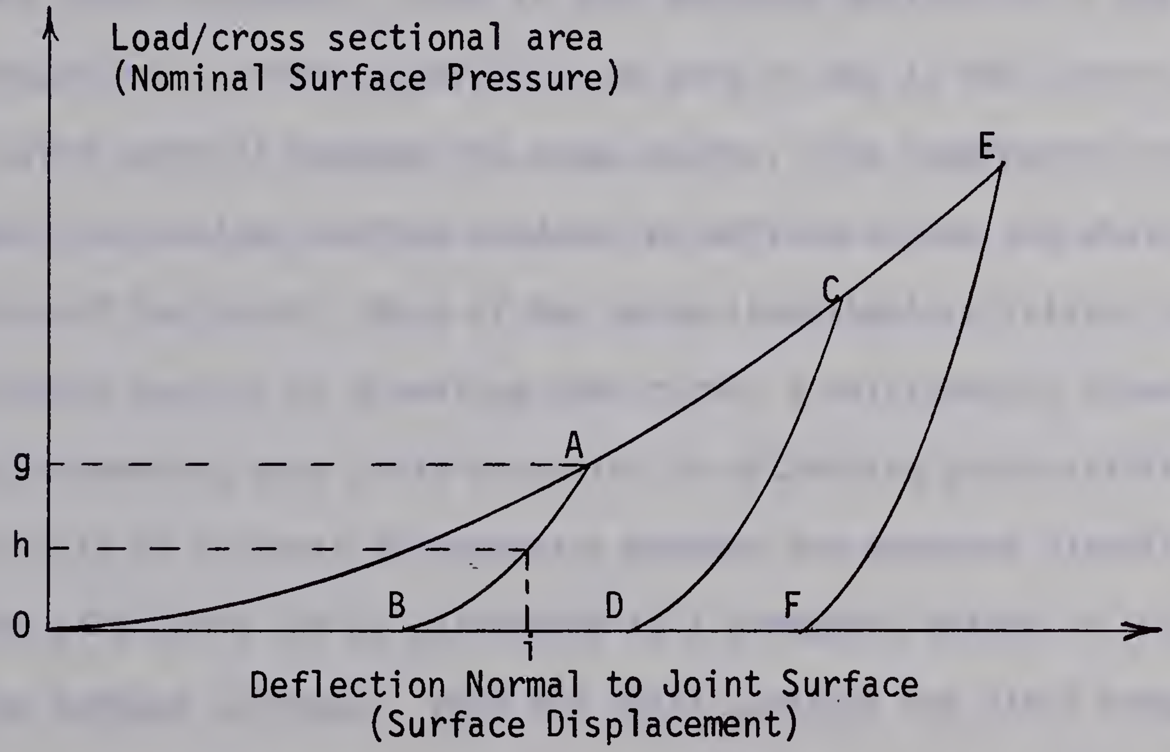

Figure 1-3 General Shape of Loading Envelope

After examining joints of various machined surfaces, Thornley et al. [5] concluded that surface roughness affects the stiffness of a joint up to some minimum surface pressure. However, they reported that this minimum surface pressure is often less than that caused by the clamping forces in machine tool joints.

In another publication Connolly and Thornley [6] attempted to relate the CLA values and deflections of joints formed by two steel specimens machined with a single point cutting tool. The specimens were the same size and shape as those used in [5]. Empirical relationships between the CLA values for the contact surfaces and the total and recoverable deflections were obtained for joints with shaped and turned contact surfaces.

Previous investigations, Ling [4], Thornley et al. [5], [6], have measured joint deflection between gauge points on the outside surfaces of the joint specimens. Part of this measured deflection is due to deformation of surface asperities and part is due to the strain in the solid material between the gauge points. The compressive strain beneath the contact surface need not be uniform across the whole cross section of the joint. None of the above investigators related load deflection results to a bearing area curve; a relationship between load and bearing area could be useful in estimating joint stiffness. It is also of interest to determine whether the measured plastic deformation of a joint can be attributed to a permanent change in the profile of the contact surfaces. When two joint surfaces are first brought together, contact is not uniform; the load is concentrated at the tips of a few surface asperities. As the load is increased these asperities

must deform or be displaced if other parts of the surface are to make contact. Kragelsky and Demkin [2] have shown by experiment that the number of points of contact increases with load, and the load deflection results of Thornley et al. [5], [6] indicated considerable plastic deformation. However, Thornley et al. [5] were unable to detect a change in the surface profile of a joint surface subjected to normal load. A permanent rearrangement of material near the contact surface could affect the elastic behavior of a joint. If the recoverable deformation curve is affected by the loading history of a joint, then it may be possible by means of large preloads to increase the stiffness of a joint without altering the load under which it operates.

1.4 Aims of the Thesis

1. To examine the effect of deformation of material below the contact surface on the extensometer measurement of joint deformation.
2. To relate joint deformation obtained from strain gauge and extensometer measurements to measurements taken from surface profiles.
3. To determine whether a change in the maximum normal load affects the elastic behavior of a joint.
4. To compare these results with those of other investigators.

CHAPTER II

EXPERIMENTAL PROCEDURE AND APPARATUS

2.1 Introduction

The experimental work in this thesis was concerned with the deformation behavior of joints formed by two steel surfaces under the action of static normal load. For each of the joints studied, one surface was machined with a single point cutting tool. The other surface was finished on a surface grinder and was smooth by comparison. The largest surface asperities were confined to only one of the specimens in contact. Contact was expected to first occur between the tips of these asperities and the relatively flat surface of the ground specimen. These two surface textures were chosen because it was desirable to estimate the first points of contact from the surface profile. The deformation of the joint under load could then be related to the surface profile and changes in the surface profile. This would be more difficult to do for two surfaces of equal roughness.

This chapter describes the apparatus and procedures used for the tests on three different joints. Section 2.2 deals with methods and equipment common to all three tests. Sections 2.3 and 2.4 describe particular features of each of the tests.

2.2 Procedures Common to Tests I, II, and III

2.2-1 Nominal Surface Pressure

The joints in Tests I, II, and III were formed with two cylindrical specimens making contact with each other at one end. Compressive loads were applied to the other ends of the specimens through a swivel joint to minimize effects caused by the end surfaces of the specimens not being parallel to the compression plates on the testing machine. The nominal surface pressure (NSP) was obtained by dividing the load by the cross sectional area of the specimen. The NSP is not necessarily the true interface pressure because the true contact area is not necessarily the cross sectional area of the joint interface.

2.2-2 Surface Displacement

The deflection between points in each of the specimens was measured with two Aminco Tuckerman optical extensometers having a gauge length of one inch. They were read to the nearest 8 μ-in. The two extensometers were placed on opposite sides of the specimens as shown in Figure 2-1. Extensometer deflections included the deformation of asperities on the contact surfaces.

Strain between the gauge points on the specimens and the contact surface was obtained from four Budd electrical resistance strain gauges. (Type C6-141-B, gauge length 1/4 in.) The strain gauges were positioned halfway between the extensometer gauge point and the contact surface.

The strain gauges were separately connected in two arm bridges to a Baldwin Lima Hamilton Model 120 strain indicator. The resolution of the strain indicator was 2 μ-in./in. and the accuracy was ± 0.1% of the reading or 5 μ-in./in. whichever was larger.

The surface displacement, x, was defined to be:

$x = \delta - \varepsilon \ell$

δ = average extensometer deflection

ℓ = extensometer gauge length

ε = average strain obtained from the strain gauges. (Assumed to be the average strain over the extensometers gauge length except for a region very close to the contact surface)

Compressive loads, deflections, and strains were taken as positive. The surface displacement is a measure of the deformation occurring near the joint surfaces. It would not occur if there were no joint.

The total, permanent, and recoverable surface displacements are illustrated in Figure 1-3. The load was first increased in increments to obtain the curve, OA. After each increment, the load was held constant while the strain gauge and extensometer readings were obtained. The curve, OA, is the total surface displacement; it includes elastic and plastic deformation when the joint is loaded for the first time. After a maximum NSP of g was reached, the load was decreased in increments to obtain the recoverable displacement curve, AB. The distance B-i represents the recoverable surface displacement when the NSP was reduced from h to 0 after the joint has been under a maximum NSP of g. The distance

0-B represents the permanent surface displacement after a NSP of g.

2.2-3 Surface Texture Measurements

Surface profiles were obtained with a Rank Taylor Hobson Talysurf 4 surface measuring instrument. This instrument operated by traversing a sharply pointed diamond stylus across the surface of a specimen. The vertical displacements of the stylus relative to some datum were magnified and recorded on a graph or were numerically assessed on an "average meter". The "average meter" gave the CLA values at one of three possible cut-off lengths, 0.01, 0.03, or 0.10 inches. The instrument had eight magnification ranges from 500 to 100,000. The overall recording accuracy for both the profile graph and the average meter was better than three percent of full scale, which on the most sensitive scale of the profile recorder (full scale = 20 μ-in.) meant an accuracy of ± 0.6 μ-in.

A sketch of the two types of datum, the rounded skid and the straight-line unit is given in Figure 2-2. The straight-line unit provided a datum that was not dependent on the surface of the specimen and was used to obtain all surface profiles in Tests I, II, and III and the CLA values of the rough specimens in Tests I and III. The rounded skid was recommended for fine textured surfaces only and was used to obtain CLA values for the ground specimens.

The CLA values for the ground surfaces were dependent on the cut-off length. They ranged from 3.5 μ-in. at 0.01 in. cut-off to 9.0 μ-in. at 0.1 in. cut-off. The scratch marks produced by the stone that made up the primary texture were spaced closer together than the irregularities

that made up the secondary texture. As the cut-off length was increased, more of the secondary texture was taken into account and the CLA values increased. Although the topography of the ground specimens was irregular, their profiles showed their surface irregularities to be small compared with those on the shaped and turned surfaces.

2.2-4 Bearing Area

Bearing area curves were obtained from the surface profiles of the rough specimens in Tests I, II, and III. The nominal surface pressure, P(x), was taken from surface displacement curves and plotted as a function of the bearing area, A(x). In P(x), x was taken to be the surface displacement, while in A(x), x was the distance into the surface from the highest point on the profile record.

2.3 Test I

The specimens in Test I were similar in size and shape to those used by Thornley et al. [5], [6]. The rough surface in Test I was produced on a shaper and strain gauges were applied to both specimens. Specifications for the specimens in Test I are given in Table 2-1:

Table 2-1 Joint Specimens Test I

O.D.	1.884 in.
I.D.	1.000 in.
Length	1 3/4 in.
Cross Sectional Area	2 square in.
Material	2 in. O.D. Cold rolled steel AISI 1018
Feed (shaped specimen)	0.012 in.
Depth of cut (shaped specimen)	0.010 in.

The specimens were joined with a split pin to prevent transverse movement and loaded on a 400,000 lb. Tinus Olsen testing machine. (Accurate to 0.1% of full scale or 0.25% of reading). For the load range used in Test I, 0 - 40,000 lb., the load could be read to the nearest 25 lb.

For each point shown on the surface displacement curves in Chapter III, the load was held constant while readings were taken for the extensometers and strain gauges. All of the loading in Test I was completed without separating the joint surfaces or removing the specimens from the testing machine.

2.4 Tests II and III

A profile of the shaped surface in Test I showed that the spacing of the surface asperities and the level of their tips was irregular. Individual tool marks could not be identified. More care was taken in Tests II and III to produce tool marks that were of a more uniform size

and shape so that information provided by the stylus instrument would be more representative of the whole contact surface.

Both of the rough specimens in Tests II and III were turned on a lathe. A Kennametal carbide tool bit with a tip radius of 1/32 in. was used on both the turned surfaces (Type K45, TNMP - 332). The most prominent feature of the surface profile was the circular arc left by the tool. Geometrical restrictions and a theoretical method for obtaining the bearing area for this type of profile are given in Appendix A.

The feed rates and machining speeds were the only controllable machining factors that were altered for the two turned specimens. The feed rate controlled the number and size of the tool marks on the workpiece. The machining speed and feed rate determined how closely the tool marks followed the profile of the cutting tool.

Ansell and Taylor [7] have compared measured with theoretical CLA values for "0.4% plain carbon steel". Their measured values were obtained from a Talysurf stylus instrument and the theoretical values were based on the feed rate and tool radius. They found that at lower machining speeds and feed rates the measured CLA values were greater than the theoretical values. As the machining speed and feed rate increased the difference between measured and theoretical values decreased.

The turned specimens in Tests II and III were machined at the maximum permissible speeds for the available equipment. The machining speeds, feed rates and depth of cut are given in Table 2-2. The shape and dimensions of the specimens are given in Figure 2-3.

Table 2-2 Machining Conditions for Turned Surfaces

	Test II	Test III
Feed rate, in./rev.	0.028	0.010
Spindle speed, rpm	370	1200
Average machining speed, fpm	120	400
Depth of cut, in.	0.005	0.005

The CLA values for the shaped specimen in Test I and the turned specimen in Test III were obtained with a Talysurf 4; however, the available magnification for the roughness meter on this instrument was too large for measuring the CLA value of the turned specimen in Test II. A CLA value of 800 μ-in. was obtained from the formula used by Ansell and Taylor [7].

$$\text{CLA} = F^2/18\sqrt{3}\ R \qquad \text{(derived in Appendix A)}$$

F = feed rate

R = tool radius

The CLA value for the turned specimen in Test II was checked with a Brüel and Kjaer roughness meter, type 6102, which gave a value of 750 μ-in. at the maximum available cut-off length, 0.058 in. This stylus instrument uses a curved skid type of datum and its resolution was greater than 50 μ-in. on the magnification range used.

A method was developed to position a specimen on the Talysurf table. A jig was made to drill 1/8 in. diameter locating holes in the base of each specimen. A specimen mount was built to fit the Talysurf table. The top surface of the mount was ground flat and locating holes were

drilled in line with the direction of the stylus traverse. Two pins were used to locate the specimen on the mount. A profile of the same traverse line could then be examined before and after loading. Figure 2-4 is a photograph showing the relative positions of the stylus, mount, specimen and straight-line datum unit.

A scratch was machined on the outer cylindrical surface of each specimen in Tests II and III, 0.500 in. from the contact surface. The scratches were used as gauge marks for the optical extensometers.

The cross sectional area of the specimens in Tests II and III was one square inch, half that used for Test I. The smaller cross sectional area reduced the number of tool marks on the surface and increased the possibility of finding deformed asperities with a stylus. It also permitted the use of a 22,000 lb. capacity Amsler testing machine for loading. The Amsler machine had a more convenient location and size than the Tinus Olsen for setting up and reading the optical extensometers. Two load ranges were used on the Amsler machine, 0 - 4400 lb. and 0 - 22,000 lb. on which the load could be read to the nearest 5 lb. and 25 lb. respectively. By calibration with a proving ring the Amsler machine was found to be accurate within ± 5 lb. or ± 0.5% of the reading on the 0 - 4400 lb. range and within ± 10 lb. or ± 0.4% of the reading on the 0 - 22,000 lb. range.

Figure 2-5 shows the loading set up for two specimens in the Amsler testing machine. The specimens in the photograph were being loaded through brass rings of the same cross section as the contact surfaces. This was done to avoid bending caused by the load being distributed over the entire end surface of the specimen.

In Tests II and III the permanent surface displacement was obtained

after each set of total displacement readings by removing most of the load. To avoid effects caused by imperfect specimen alignment the load was not completely removed. For Test II the minimum load was between 0 and 5 lb. on the 4400 lb. range and between 0 and 25 lb. on the 22,000 lb. range. For Test III the minimum loads were fixed at 10 lb. on the 4400 lb. range and 50 lb. on the 22,000 lb. range.

As in Test I, the surface displacement results for Tests II and III were obtained by holding the load constant while readings for the extensometers and strain gauges were taken. However, the specimens in Tests II and III were removed from the testing machine twice during each test to examine the surface profiles, after a maximum NSP of 4000 and 10,000 psi.

The procedures outlined in this chapter were used to obtain the results discussed in Chapter III.

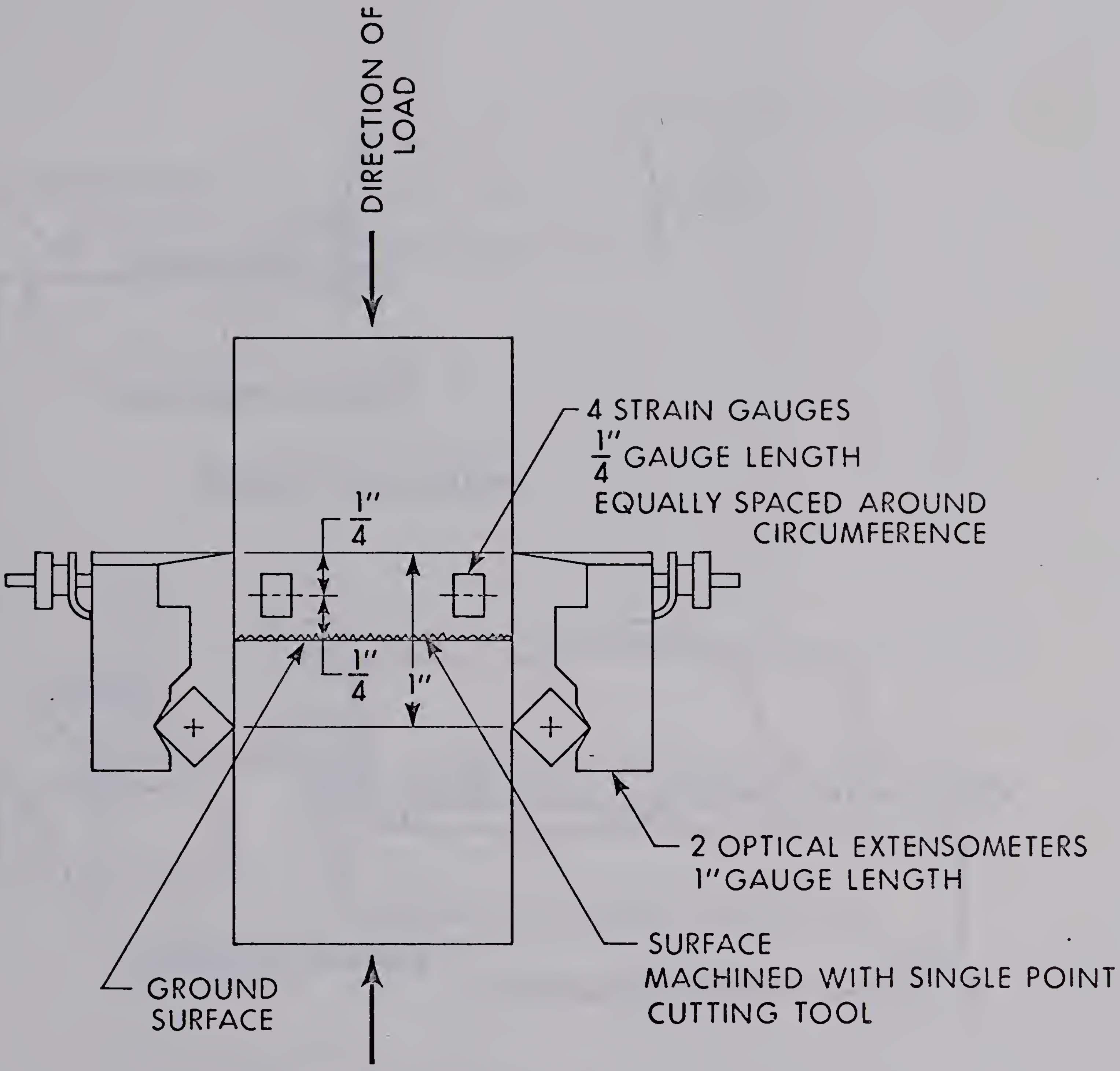

Figure 2-1 Arrangement of Extensometers and Strain Gauges

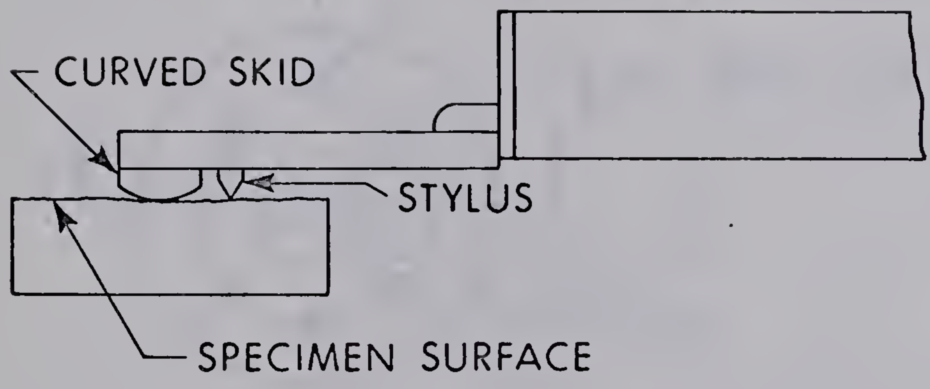

CURVED SKID DATUM

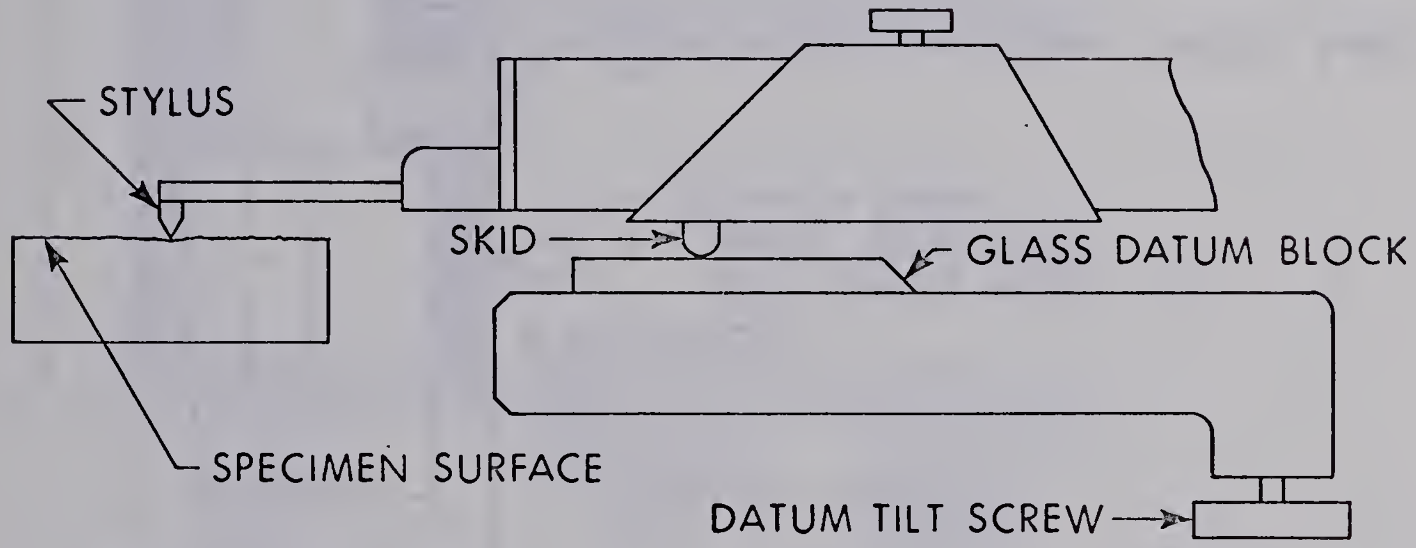

STRAIGHT LINE UNIT DATUM

Figure 2-2 Datum for Surface Measuring Instrument

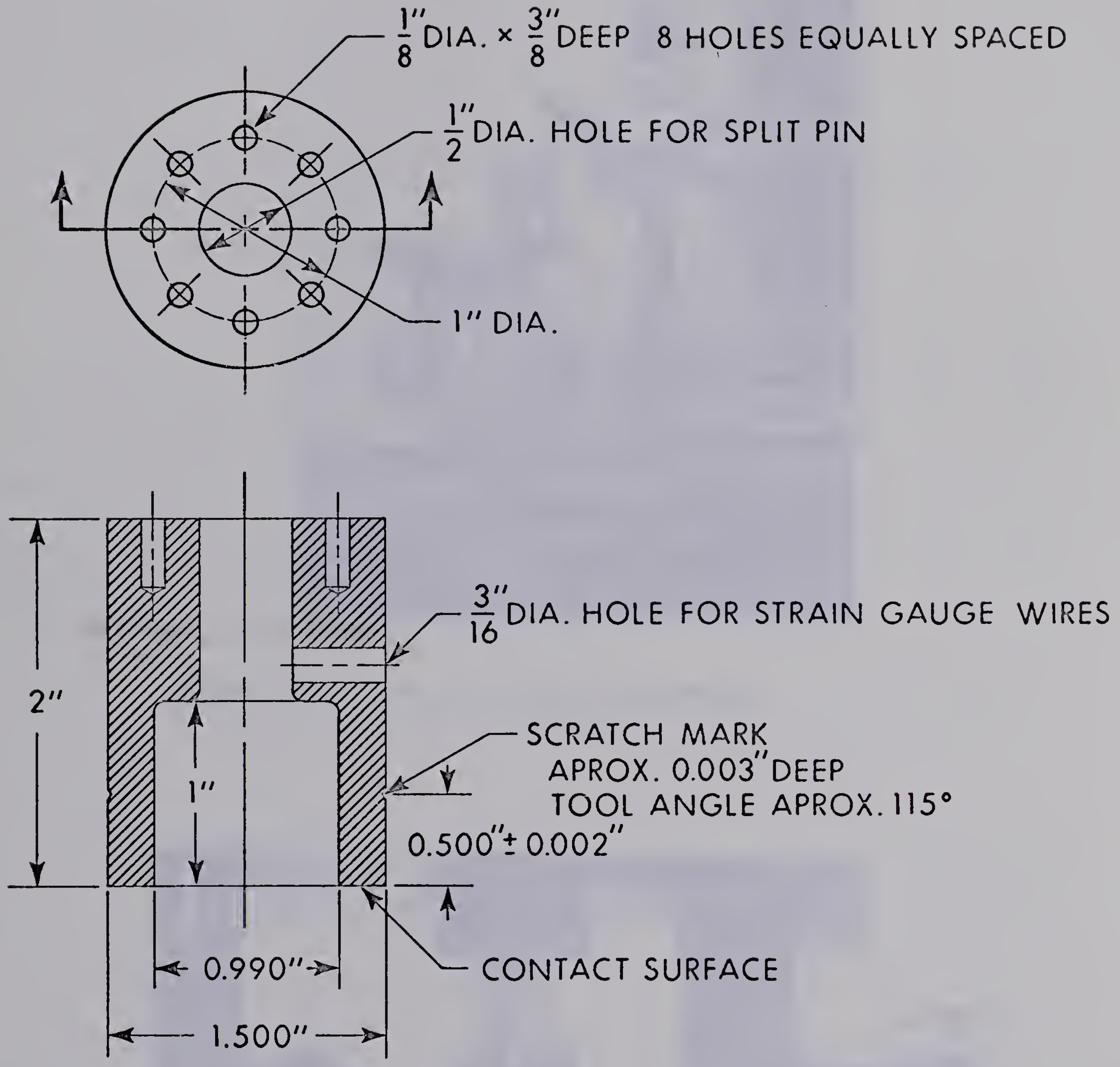

MATERIAL: 1 1/2" DIA. GROUND STEEL A.I.S.I. 1045

SCALE: FULL

Figure 2-3 Joint Specimen, Tests II and III

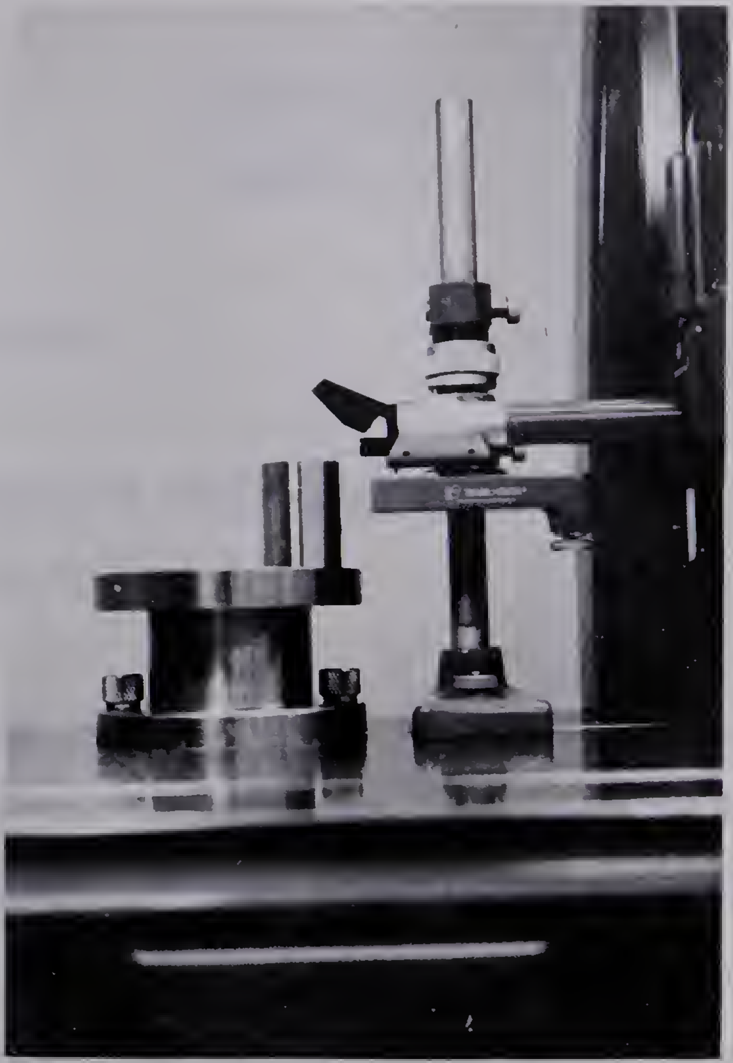

Figure 2-4 Surface Profile Measurement

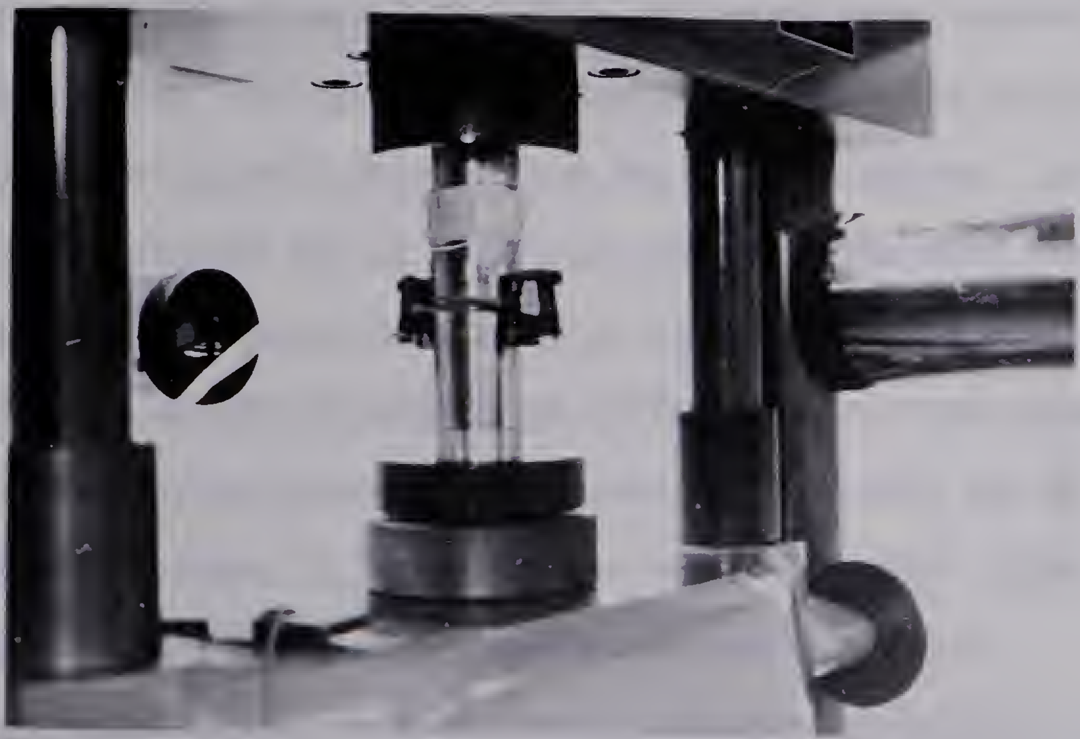

Figure 2-5 Loading Arrangement

CHAPTER III

RESULTS

3.1 Strain Gauge Results

3.1-1 Differences in Strain Gauge Results Between the Two Specimens in Test I

The strain gauge results for Test I, Figure 3-1, indicated significant differences in strain at different locations around the circumference of either specimen. However, the difference in average strain values between the two specimens (Table 3-1) was small. Strain gauges were applied to one specimen only for Tests II and III.

3.1-2 Differences in Strain Gauge Results for Test II

For Test II all of the strain gauge and extensometer readings up to a maximum NSP of 4000 psi were taken without separating the joint surfaces or removing the specimens from the testing machine. For the loading up to a maximum NSP of 10,000 psi the specimens were rotated ninety degrees with respect to a vertical axis in the testing machine. This was done to determine whether the differences in strain gauge readings around the circumference of the turned specimen were due to eccentric loading. As shown in Table 3-2 the individual strain gauge results changed, but the changes did not indicate eccentric loading.

Strain gauge results from the inner and outer cylindrical surfaces

of the turned specimen in Test II are shown in Figure 3-2. The large differences between average strain values on the inner and outer surfaces indicated that the strain between the extensometer gauge points was not uniform across the thickness of the specimen. Because the extensometers measured deflections between gauge marks on the outer surface of the specimens, average strain on the outer surface only was used to calculate surface displacement.

The average strain on the inside cylindrical surface of the turned specimen in Test II was significantly larger than the average strain on the outside surface. For the loading up to a maximum NSP of 20,000 psi the specimens were placed in their original position in the testing machine but were loaded through brass rings of the same cross section as the contact surfaces. This was done to avoid bending caused by the load being distributed over the entire end surface of the specimen. Average strain gauge results for Test II are compared in Table 3-5; although these results did not indicate that bending had occurred in Test II up to 10,000 psi, the brass rings were used for all of Test III.

Along with eccentric loading and bending, there are two other possible causes for changes in individual strain gauge results: a difference in the relative positions of the specimens after they had been separated and brought into contact again, or a change in the load distribution across the contact surface with a change in the maximum load.

3.1-3 Check on the Strain Gradient

The strain gradient in the axial direction was checked on the turned

specimen in Test II. Three 1/16 inch Budd strain gauges (type C6-111) were placed in line between the turned surface and the extensometer gauge mark. For a clean contact surface, the strain gradient as shown in Figure 3-4a was negligible; however, it was affected by debris on the contact surface. The gradient shown in Figure 3-4b was produced by a small piece of cellulose tape on the contact surface and in line with the three strain gauges.

3.1-4 The Effect of Strain Obtained from Strain Gauges on the Extensometer Deflection

Kragelsky and Demkin [2] have reported that the number of asperities in contact and the size of their contact areas increases with load. This would cause the overall stiffness of a joint to increase with load while the stiffness of the solid material in the joint specimen would remain constant for loads not exceeding the proportional limit.

Figures 3-5, 3-6, and 3-7 show the effect of deflection obtained from the strain gauge results on deflection measured by the extensometers ($\varepsilon\ell/\delta \times 100\%$ as a function of NSP). The extensometers measured deflections between two gauge marks, one on each specimen, and included the deformation of surface asperities. The stiffness increased with load as indicated by the extensometers and the effect $\varepsilon\ell/\delta$ also increased with load.

Strain in the material beneath the contact surfaces affected the recoverable extensometer deflection more than the total deflection. The

total deflection included plastic deformation of the surface asperities. After a loading sequence, no permanent strain was indicated by the strain gauges.

3.1-5 The Effect of Strain on the Recoverable Surface Displacement

As shown in Figures 3-1, 3-2, and 3-3, individual strain gauge readings did not vary linearly with the NSP over the entire load range. Differences in individual strain gauge readings indicated the uneveness of the load distribution at the contact surface.

Figure 3-8 gives the average strain gauge results from the outer cylindrical surface of the specimens in Tests I, II, and III. The ordinate for the dashed line is the NSP divided by the modulus of elasticity of steel, taken to be 30 x 10^6 psi.

Figure 3-9 compares the extensometer deflection with recoverable surface displacement. The surface displacement was obtained by subtracting the average strain gauge readings (Figure 3-8) multiplied by the extensometer gauge length from the extensometer readings.

$$x = \delta - \varepsilon \ell$$

The dashed lines in Figure 3-9 represent recoverable surface displacement assuming a uniform strain over the cross section of the specimens equal to that given by the dashed line in Figure 3-8. As shown in Figure 3-9, this assumption had a noticeable effect in Tests I and II. Therefore, the surface displacement results for all three tests were based on the average strain gauge results from the outer cylindrical surface of the

joint specimens. A complete set of strain gauge readings was taken for each set of extensometer readings.

The differences between the solid and dashed curves in Figure 3-9 indicate that surface displacement is sensitive to measurement techniques. Thornley et al. [5] suggested that joint deflection caused by irregular topography of the contact surfaces be determined as the deflection across the joint surface less the deflection of an "equivalent solid piece". The strain gauge results in Tests I, II, and III showed that the compressive strains normal to the contact surfaces were not uniform over the cross sections of the joint specimens. Thus, the method suggested by Connolly et al. cannot be taken to imply that the strain at the outer surface of the joint specimens (i.e. where the extensometer measurements are taken) is the same as in the equivalent solid piece. Their method could also impose serious practical difficulties in constructing an equivalent solid component, especially if the joint in question were composed of two dissimilar materials.

3.2 General Shape of the Loading Envelopes

The loading envelopes shown in Figures 3-10, 3-11, and 3-12 were similar to those reported by Thornley et al. [5], [6]. The stiffness of the joints when loaded for the first time increased with load as indicated by the total displacement curves. The total surface displacement included both elastic and plastic deformation. The slopes of the recoverable displacement curves also increased with load. The permanent displacement curves in Figures 3-11 and 3-12 are a measure of the plastic

deformation when the joints were loaded for the first time.

3.3 Total and Permanent Surface Displacement Results

Total and permanent surface displacement curves for Tests II and III are presented in Figures 3-13 and 3-14. Both permanent and total displacements were greater for Test II than Test III. In Figures 3-10 and 3-11 the permanent and total surface displacements are compared; for Test II the permanent displacement was a larger part of the total displacement than for Test III.

The differences in surface displacement results between Tests II and III were caused by differences in the surface topography of the turned specimens. Both of the turned specimens were prepared on the same lathe and with the same tool, but the feed rates and machining speeds were different. The most prominent feature of their surface profiles was the circular arc left by the tool. The most noticeable differences in the two specimens was the height and spacing of the tool marks. The turned specimen in Test II had fewer tool marks (i.e., grooves which could be identified with the shape of the cutting tool) than in Test III and the load was concentrated at fewer points.

The total surface displacement results were compared with an empirical relationship obtained by Connolly and Thornley [6]. These authors have suggested that, for shaped, planed, or turned surfaces, the total deflection at a given load is directly proportional to the CLA value for the contact surfaces, that is, $\lambda = z \times \text{CLA}$, where z is a function of P, the nominal surface pressure. An experimental curve

of P as a function of z was given by Connolly and Thornley [6] and is explained in more detail in Appendix B. Their results were obtained from several mild steel specimens machined on different machine tools.

In obtaining the function, z, Connolly and Thornley referred their results to the deflection at 10 tons/in.^{2} (22,400 psi). Figures 3-15 and 3-16 compare the total surface displacements for Tests I, II, and III to the curves z × CLA. The maximum NSP applied in Tests I, II, and III was 20,000 psi and the total surface displacement at this NSP was used as a datum for the comparison.

Connolly and Thornley obtained their results from joints of like machined surfaces of equal roughness. In each of Tests I, II, and III one of the joint specimens was turned or shaped and the other was ground. The profile irregularities and the CLA values of the ground specimens were small compared to the tool marks and CLA values of the shaped and turned specimens. A joint formed by one rough surface and one smooth surface was expected to have a higher stiffness than one formed by two rough surfaces. This was not indicated for the entire load range by the curves compared in Figures 3-15 and 3-16.

The use of one smooth surface, differences in material properties, and different methods of determining surface displacement could have caused some of the differences between the experimental and empirical results in Figures 3-15 and 3-16. However, it is unlikely that the surface geometry of the joint surfaces was sufficiently specified by the type of machining operation and a CLA value. The CLA value includes only the topography that falls within the cut-off length on a particular stylus traverse and in some cases is insensitive to changes in surface

profile within the cut-off length. Therefore, if the formula $\lambda = z \times CLA$ is to be valid, the function z must take into account a range of geometrical configurations within the cut-off length as well as profile irregularities that are not included in the CLA value.

3.4 Permanent Change in Surface Profile with Load

The total and permanent surface displacements for Tests II and III were much larger than those observed from the surface profiles. Thornley, Connolly, Barash and Koenigsberger [5] have reported profile changes of a shaped mild steel specimen pressed against a lapped hardened steel block. The height of the tool marks on their shaped specimen was about 700 μ-in. They noticed very little change in the surface profile below 35 tons/in.^{2} (78,400 psi) nominal surface pressure, and have suggested that plastic deformation takes place mainly below the surface.

For Tests II and III, profile records were taken of both mating surfaces. Surface profiles of the turned and ground specimens after nominal surface pressures of 0, 4,000, 10,000 and 20,000 psi are given in Figures 3-17 to 3-20. The tool marks on the turned specimen in Test III were about the same height and spacing as those on the shaped specimen used by Thornley et al [5], and there was no obvious change in the profile with load. The change in profile with load in Test II was more evident for both the turned and ground specimens.

The turned specimen in Test II had fewer and larger tool marks and there was a greater difference in the level of the peaks than for the turned specimen in Test III. The load was less uniformly distributed

across the contact surface in Test II, and the asperities observed on the surface profile were supporting a larger proportion of the load. Because the turned surface in Test II had fewer tool marks than Test III, there was more chance of the stylus traversing asperities that had undergone noticeable permanent deformation on the turned surface and permanent indentations on the ground surface.

For Test II, the noticeable change in the height of the tool marks on the turned surface and the depth of the indentations on the ground surface was small compared to the permanent displacement measured by the extensometers up to a nominal surface pressure of 4,000 psi. At these loads there were probably very few asperities making contact with the mating surface and the stylus did not traverse across them. However, after maximum nominal surface pressures of 10,000 and 20,000 psi, profile changes in Test II were more noticeable. Figure 3-21 compares the change in profile with the change in permanent surface displacement after a NSP of 4,000 psi. The change in profile was taken to be the sum of the average change in the maximum height of the tool marks plus the average change in the maximum depth of the indentations on the ground surface. The maximum height of the tool marks was taken as the maximum vertical distance between two points on any given profile record. The height of the tool marks was measured on the chart to the nearest 20 μ-in., the depth of the indentations to the nearest 10 μ-in. Four profiles from different positions on each specimen were taken and the average changes are given in Table 3-3.

3.5 Bearing Area Results

Bearing area curves for the turned specimen in Test II are shown in Figure 3-22. The experimental points were obtained from four different profile records. A common datum was chosen by graphically extrapolating each set of experimental points through zero bearing area. The dashed line is a theoretical curve based on the feed rate, F, and the tool radius, R.

$$A = 1 - 2/F \sqrt{F^2/4 - 2x\sqrt{R^2 - F^2/4} - x^2}$$

The distance into the surface from the tip of the tool marks is x. This formula is derived in Appendix A. The differences between the theoretical curve and experimental points were caused mainly by variations in the level of the tips and bottoms of the tool marks.

Nominal surface pressures, P(x), from the total and permanent displacement curves for Tests II and III were plotted as functions of bearing area, A(x), in Figure 3-23. In A(x), x was the distance into the surface from the point of zero bearing area; in P(x), x was the surface displacement. These curves cannot be accepted as a true indication of the stiffness of a joint under normal load because for P(x) and A(x) to be referred to the same datum, the bearing area curve must come from a representative surface profile that contains the first points that come into contact with the mating surface. The permanent change in surface profile with load was not noticeable in Test III and only after loads that had caused large total and permanent surface displacements in Test II. Since the bearing area curves were taken from these surface

profiles, they probably did not contain the first points to make contact.

3.6 Recoverable Surface Displacement Results

Connolly and Thornley [6] suggested that loading history does not affect the elastic recovery of a joint and that unloading curves are congruent over the same load range. The recoverable displacement curves for Test I, Figure 3-24, indicate this may not be true for all machined surfaces. The difference in the average strain values used for the recoverable displacement curves, Table 3-4, were small compared to the difference in recoverable surface displacement.

The recoverable displacement curves for Test I are shown with the total surface displacement in Figure 3-10. Figure 3-10 indicates considerable permanent surface displacement had taken place between 2,000 and 20,000 psi maximum NSP. The permanent surface displacement measured by the extensometers was probably due to plastic deformation at or near regions of contact. Plastic deformation could alter the unloaded positions of these regions in the direction of the load. If the contact regions were redistributed over a smaller interval in the direction of the load, the elastic stiffness of the joint would increase.

The change in recoverable displacement curves with an increase in the maximum NSP was not as noticeable for Test II as Test I. The asperities on the shaped surface in Test I were irregular in size and shape compared to the tool marks on the turned specimen in Test II.

Figure 3-25 indicates a small increase in stiffness with an increase in maximum NSP for Test II. However, the differences in these recoverable

displacement curves when referred to a datum of 500 psi was insignificant as shown in Figure 3-26. Also shown in Figure 3-26 are the recoverable surface displacement curves after maximum NSP of 10,000 and 20,000 psi. The differences between recoverable displacement curves after 4,000, 10,000, and 20,000 psi maximum NSP were the same order of magnitude as the differences in the strain gauge results, Table 3-5.

Recoverable displacement curves for Test III are shown in Figures 3-27 and 3-28. Strain gauge results used for Figure 3-28 are given in Table 3-6. Figure 3-27 indicates a significant decrease in recoverable surface displacement with an increase in the maximum NSP. The differences in the recoverable surface displacement curves referred to a datum of 100 psi, Figure 3-28, were much smaller, but these curves still indicate a decrease in recoverable surface displacement with an increase in maximum NSP.

Connolly and Thornley [6] suggested that the elastic stiffness of a joint in the direction normal to the contact surfaces is directly proportional to the normal load. They reported the following relation for the normal elastic deflection of a joint:

$$\ln P/P_0 = m\,\lambda$$

The nominal surface pressure is P and λ is the change in normal deflection corresponding to a change in NSP of $P - P_0$. The constant, m, depends on material properties and the topography of the joint surfaces.

The valid range of the above expression was reported as: 0.05 tons/in.^{2} (114 psi) to 2.5 tons/in.^{2} (5,600 psi) for shaped surfaces and 0.05 tons/in.^{2} to 3 tons/in.^{2} (6,720 psi) for turned surfaces.

An approximate relation between m and CLA values for shaped and turned mild steel surfaces was given as CLA × m = Q, a constant for a given material and machining operation.

$$Q = 5.34 \quad \text{for turned surfaces}$$

$$Q = 6.42 \quad \text{for shaped surfaces}$$

Connolly and Thornley obtained their results from surfaces of equal roughness but stated that the mating of a rough and a smooth surface resulted in the same m value as a joint formed by two rough surfaces. The CLA values for Tests I, II, and III and the corresponding m values taken from [6] are given in Table 3-7. The relation $\ln P/P_o = m\lambda$ was compared with the recoverable surface displacement results in Figure 3-29, 3-30, and 3-31. The experimental points, log P/P_o, appeared to depend linearly on the recoverable surface displacement for part of the load range. However, points from different recoverable displacement curves did not fall on the same line for Tests I and III.

The slopes of the experimental curves in Figures 3-29, 3-30 and 3-31 differed from the m values obtained from the empirical relation CLA × m = Q. Connolly and Thornley's results were obtained from several specimens machined on different machine tools and their experimental m values showed a similar scatter. The differences indicate the use of an m value in predicting the recoverable surface displacement of an individual joint is not reliable. Because the results show a straight line relationship between NSP and recoverable surface displacement on semi-log paper for part of the load range, Connolly and Thornley's suggested equation should not be totally rejected. However, if the formula

is to be valid for design it must take into account parameters other than just the CLA value.

3.7 Summary of Results

Deformation of the solid material between the contact surfaces and the extensometer gauge marks, as indicated by the strain gauge results, was a significant portion of the total extensometer measurement. The irregular topography of the contact surfaces caused non uniform loading and the compressive strains normal to the contact surfaces were not uniform over the cross section of the joint specimen. Surface displacement results were affected by assuming a uniform compressive strain over the cross section of the joint specimen.

The surface topography of joint surfaces changed with normal load. Detection of the change was limited by the nature of the joint specimens and the technique used to obtain the surface profile. If profile records are obtained with a stylus type instrument, the stylus should traverse the same horizontal paths over the specimen surface each time profile recordings are made. Individual asperities or indentation marks can then be identified and their change after loading observed. This was achieved in Tests II and III with a mount affixed to the Talysurf base table. A permanent change in surface profile was evident only if the stylus traversed a part of the surface that had been loaded enough to cause noticeable plastic deformation. In Test II the permanent change in the profiles of the joint surfaces was approximately equal to permanent surface displacement after a maximum nominal surface pressure

of 4,000 psi. However, changes in profile were not as noticeable for the specimens in Test III. The turned specimen in Test III had more and smaller tool marks than Test II. This suggests that the opportunity to observe a change in profile with a stylus type instrument improves as the number of asperities on the joint surface is decreased.

Because the bearing area curves did not accurately represent the contact surfaces, bearing area was not successfully related to the surface displacement results. A bearing area curve can be made more representative of a contact surface by decreasing the number of asperities or making them uniform in size and shape. The tool marks on the turned specimens in Tests II and III were too numerous and irregular for the bearing area curves to contain the first points of contact.

The recoverable surface displacement was affected by the loading history of the joints. The elastic stiffness of the joints increased with an increase in the maximum nominal surface pressure. This change in stiffness was probably due to plastic deformation at or near regions of contact.

Significant differences were noticed between surface displacement results and the empirical relations suggested by Connolly and Thornley [6]. Specification of the type of machining operation and a CLA value were found to be an insufficient assessment of surface texture for predicting surface displacement.

Table 3-1 Difference in Strain Gauge Values After a Maximum NSP of 20,000 psi, Test I

A - Nominal surface pressure

B - Average strain from four gauges on each specimen

C - Average difference between two opposite gauges

D - Difference between two specimens in average strain

A, psi	B, μ-in./in.	C, μ-in./in.	D, μ-in./in.
500	48	10	4
1,000	94	15	0
2,500	224	9	4
5,000	339	27	26
7,500	422	11	0
10,000	514	21	1
12,500	607	17	1
15,000	692	25	0
17,500	774	36	11
20,000	859	26	5

Table 3-2 Individual Strain Gauge Results for Test II

Compressive Strain in μ-in./in.

Up to a Maximum NSP of 4,000 psi

NSP, psi	1	2	3	4	5	6	7	8
1,000	39	8	63	130	1	7	57	-8
2,000	81	30	119	197	5	37	101	1
3,000	122	64	166	248	20	72	140	13
4,000	167	100	215	293	44	108	175	26

Up to a Maximum NSP of 10,000 psi (specimen rotated 90 degrees)

NSP, psi	1	2	3	4	5	6	7	8
1,000	183	26	18	82	0	-9	13	10
2,000	248	72	55	145	14	-16	34	20
3,000	301	111	99	197	40	-19	56	53
4,000	345	148	146	239	72	-18	71	85
6,000	430	216	230	326	138	2	142	154
8,000	507	285	312	402	209	34	207	223
10,000	588	354	393	478	284	73	266	300

Up to a Maximum NSP of 20,000 psi (specimen loaded through Brass Rings)

NSP, psi	1	2	3	4	5	6	7	8
1,000	169	18	40	116	4	-9	11	-28
2,000	240	56	90	181	26	-14	36	-28
3,000	299	83	139	240	68	-10	69	-15
4,000	344	125	188	287	103	-7	103	10
6,000	430	181	278	371	168	27	174	71
8,000	507	255	348	451	240	77	244	140
10,000	579	318	424	527	308	135	312	210

Position of Specimen and Gauges

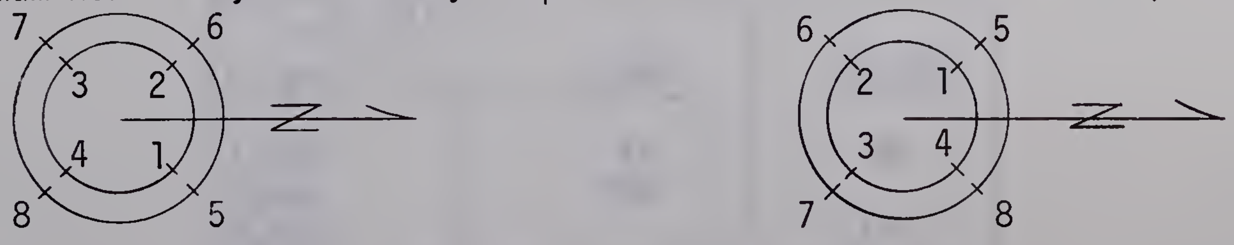

Maximum NSP of 4,000 and 20,000 psi

Maximum NSP of 10,000 psi

Table 3-3 Permanent Change in Profile after an NSP of 4,000 psi, Test II

A - Nominal surface pressure

B - Change in the maximum height of the tool marks on the turned surface

C - Change in the maximum depth of indentations on the ground surface

D - Total change (B + C)

B and C are average values taken from four different profiles

A, psi	B, μ-in.	C, μ-in.	D, μ-in.
10,000	80	190	270
20,000	200	240	440

Table 3-4 Average Strain Gauge Results used for Recoverable Surface Displacement Curves, Test I

A - Nominal surface pressure

B - Maximum NSP for the recoverable displacement curve.

Strain is the increase in average strain after a NSP of 500 psi, μ-in./in.

B, psi A, psi	2,000	20,000
1,000	48	44
2,000	142	
2,500		175

Table 3-5 Average Strain Gauge Results used for Recoverable Surface Displacement Curves, Test II

A - Nominal surface pressure

B - Maximum NSP for the recoverable displacement curve

C - Average strain from the four strain gauges on the inner surface of the turned specimen, μ-in./in.

D - Average strain from the four strain gauges on the outer surface of the turned specimen, μ-in./in.

Strain is the increase in average strain after NSP of 500 psi

B, psi / A, psi	4,000		10,000		20,000	
	C	D	C	D	C	D
1,000	28	11	27	2	36	1
2,000	75	31	80	7	92	12
3,000	118	56	127	36	140	35
4,000	162	83	170	56	186	59
6,000			250	113	265	87
8,000			327	172	340	182
10,000			403	235	412	248

Table 3-6 Average Strain Gauge Results used for Recoverable Surface Displacement Curves, Test III

A - Nominal surface pressure

B - Maximum NSP for the recoverable displacement curve

Strain is the increase in average strain after a NSP of 100 psi, μ-in./in.

B, psi A, psi	500	2,000	4,000	20,000
200	3	1	1	3
300	8	5	2	6
400	11	4	4	10
600		8	8	17
800		13	14	22
1,000		19	19	30
1,500			35	46
2,000		51	52	61
2,500			68	78
3,000			85	99
3,500			102	113
4,000			119	131

Table 3-7 CLA and m Values for the Rough Specimens in Tests I, II, III

Test	Type of Surface	CLA μ-in.	Cut-Off in.	Q	m in^{-1}
I	Shaped	225	0.10	6.42	2.85×10^4
II	Turned	800*		5.34	0.67×10^4
III	Turned	190	0.03	5.34	2.81×10^4

* Obtained from the formula:

$$\text{CLA} = F^2/18\sqrt{3}\ R$$ (derived in Appendix A)

F = feed rate

R = tool radius

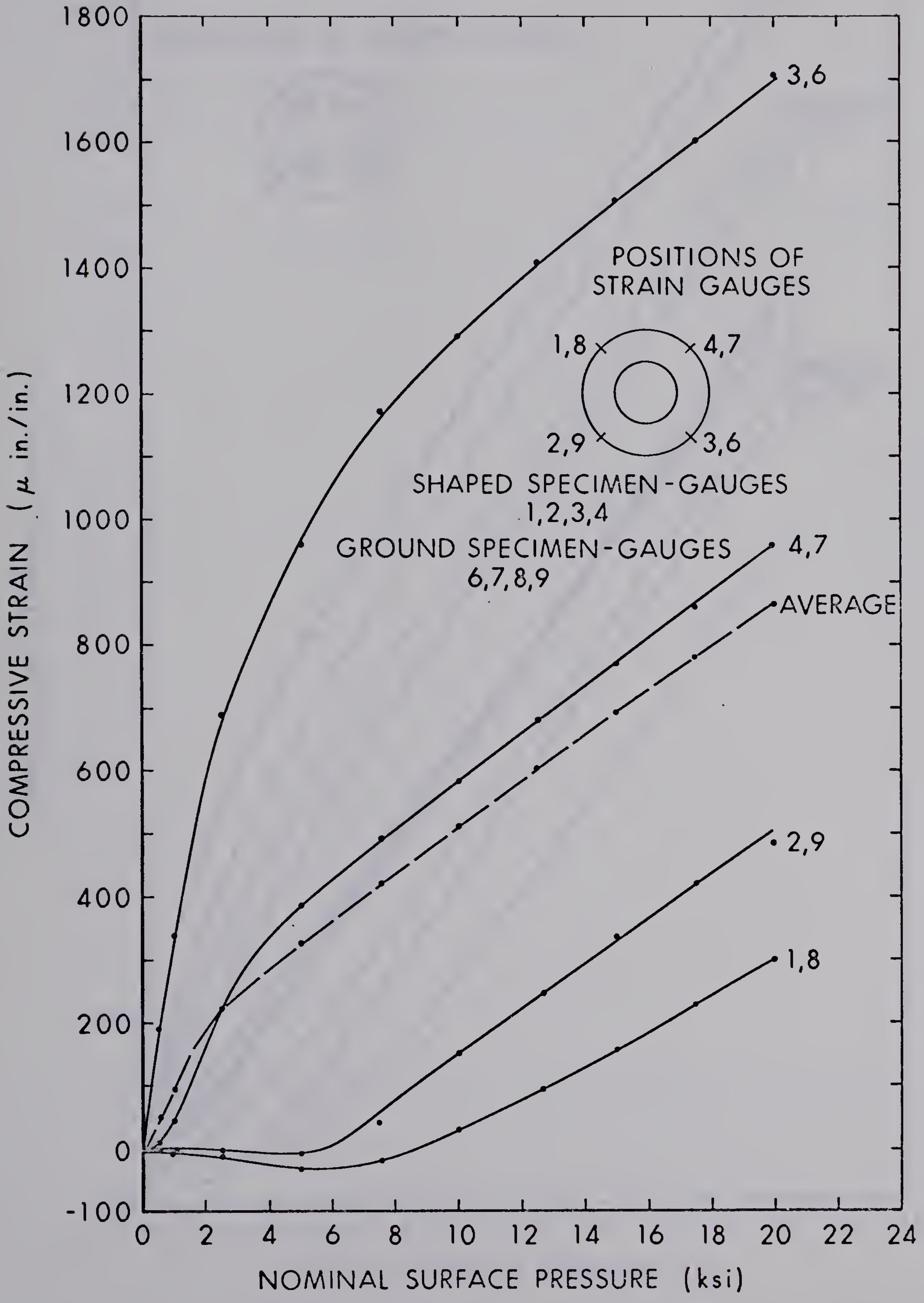

Figure 3-1 Strain Gauge Results for Test I after 20 ksi Nominal Surface Pressure

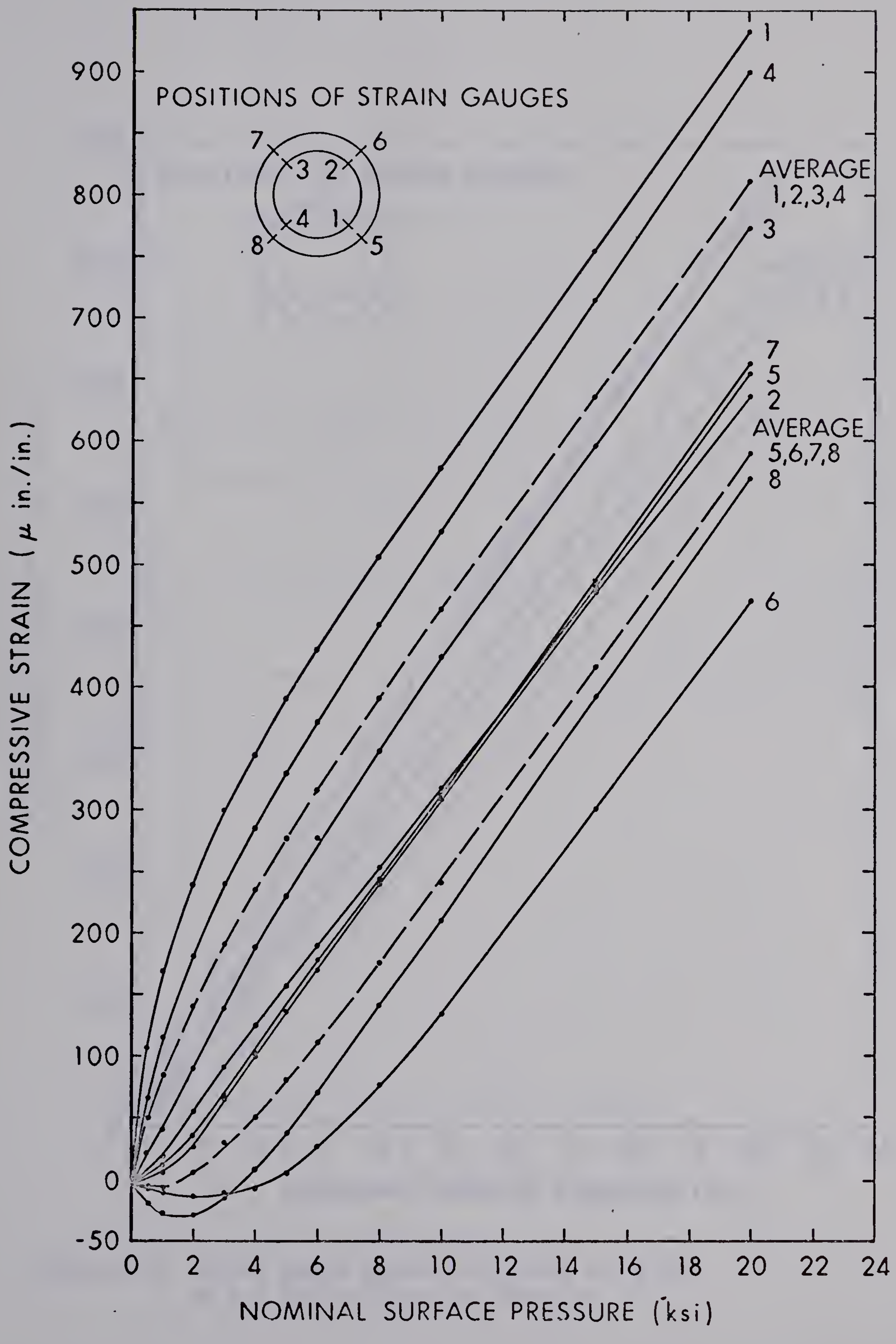

Figure 3-2 Strain Gauge Results for Test II after 20 ksi Nominal Surface Pressure

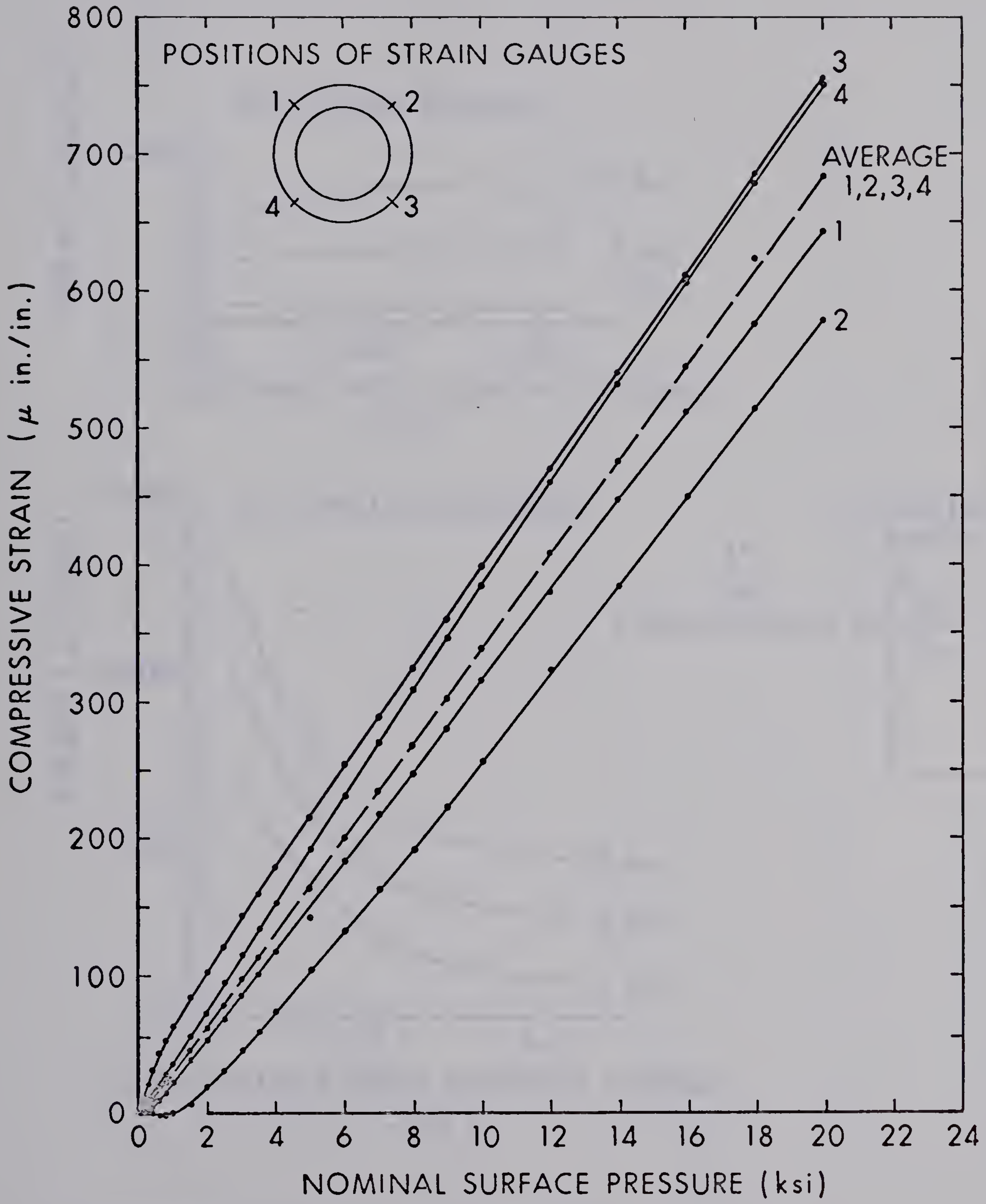

Figure 3-3 Strain Gauge Results for Test III after 20 ksi Nominal Surface Pressure

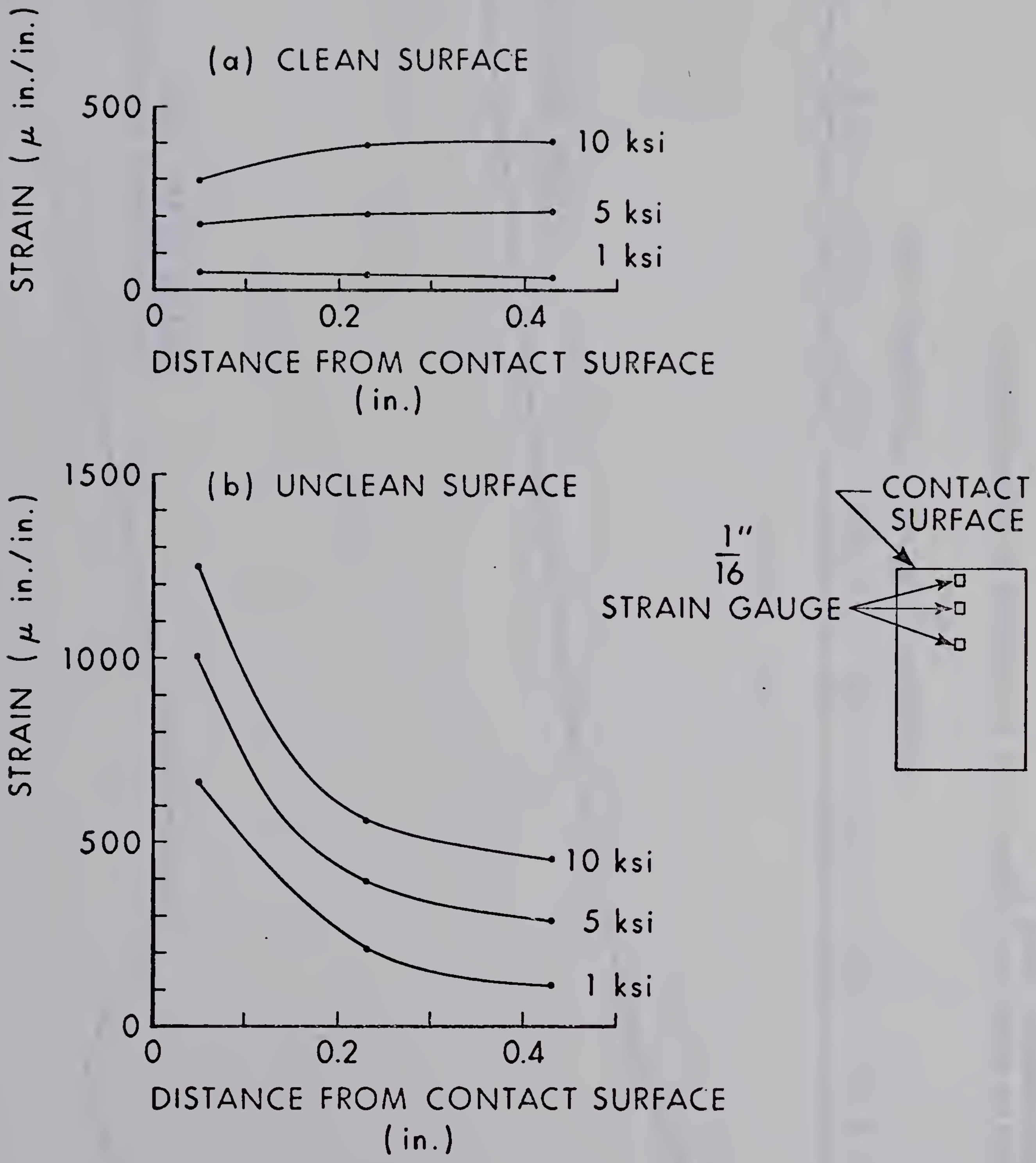

Figure 3-4 Strain Gradient Test II

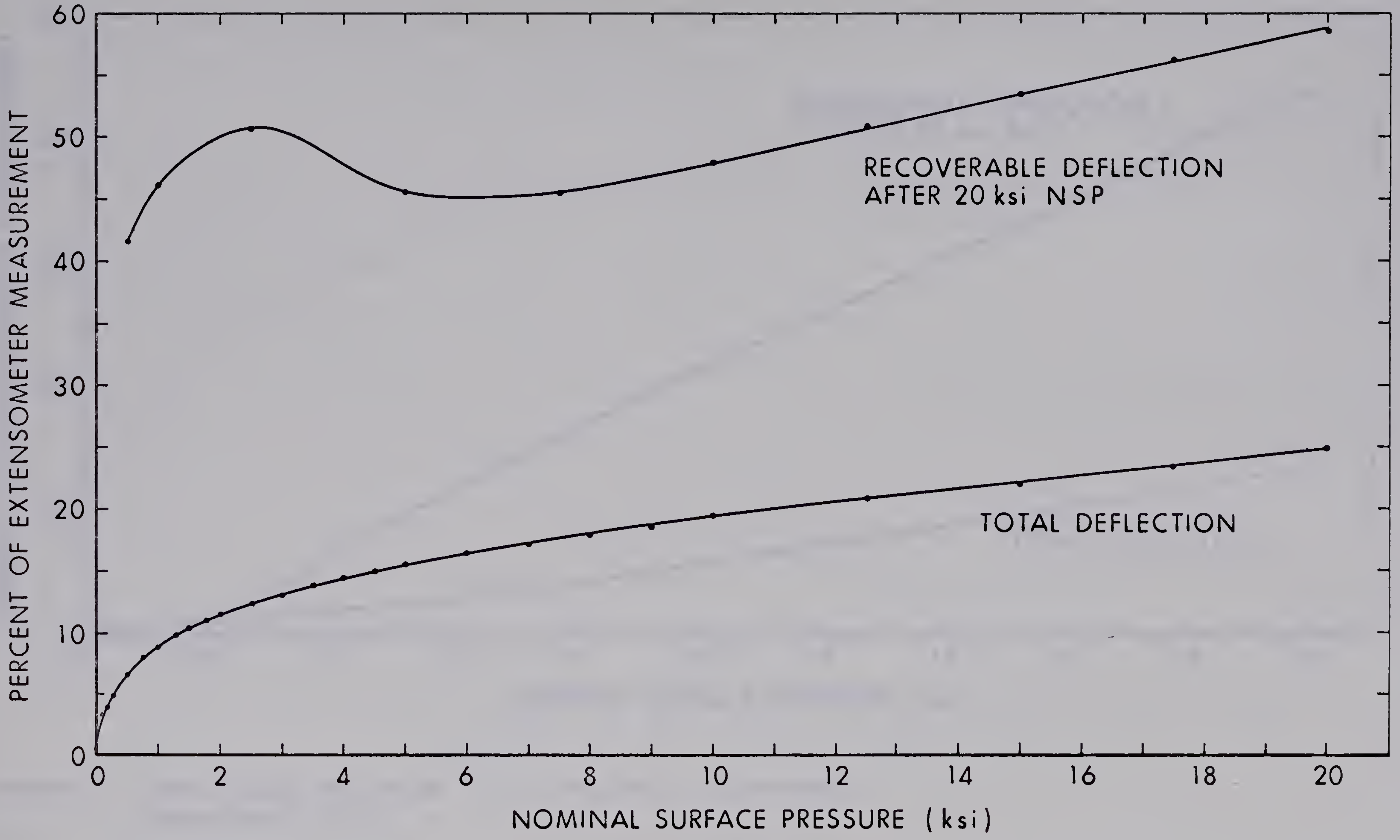

Figure 3-5 Strain Gauge Deflection ($\varepsilon \ell$) as Percent of Extensometer Measurement, Test I

[illegible]

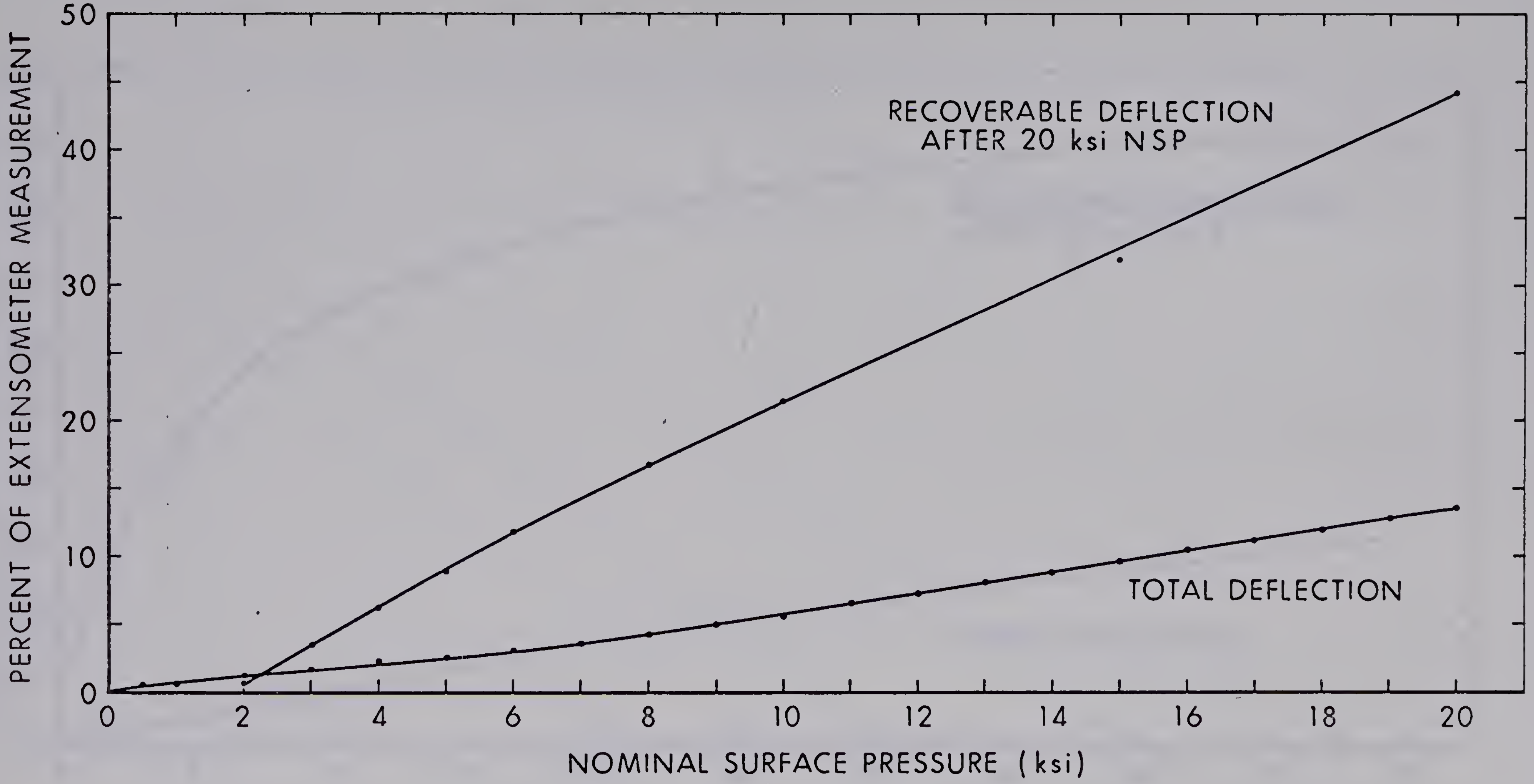

Figure 3-6 Strain Gauge Deflection (εℓ) as Percent of Extensometer Measurement, Test II

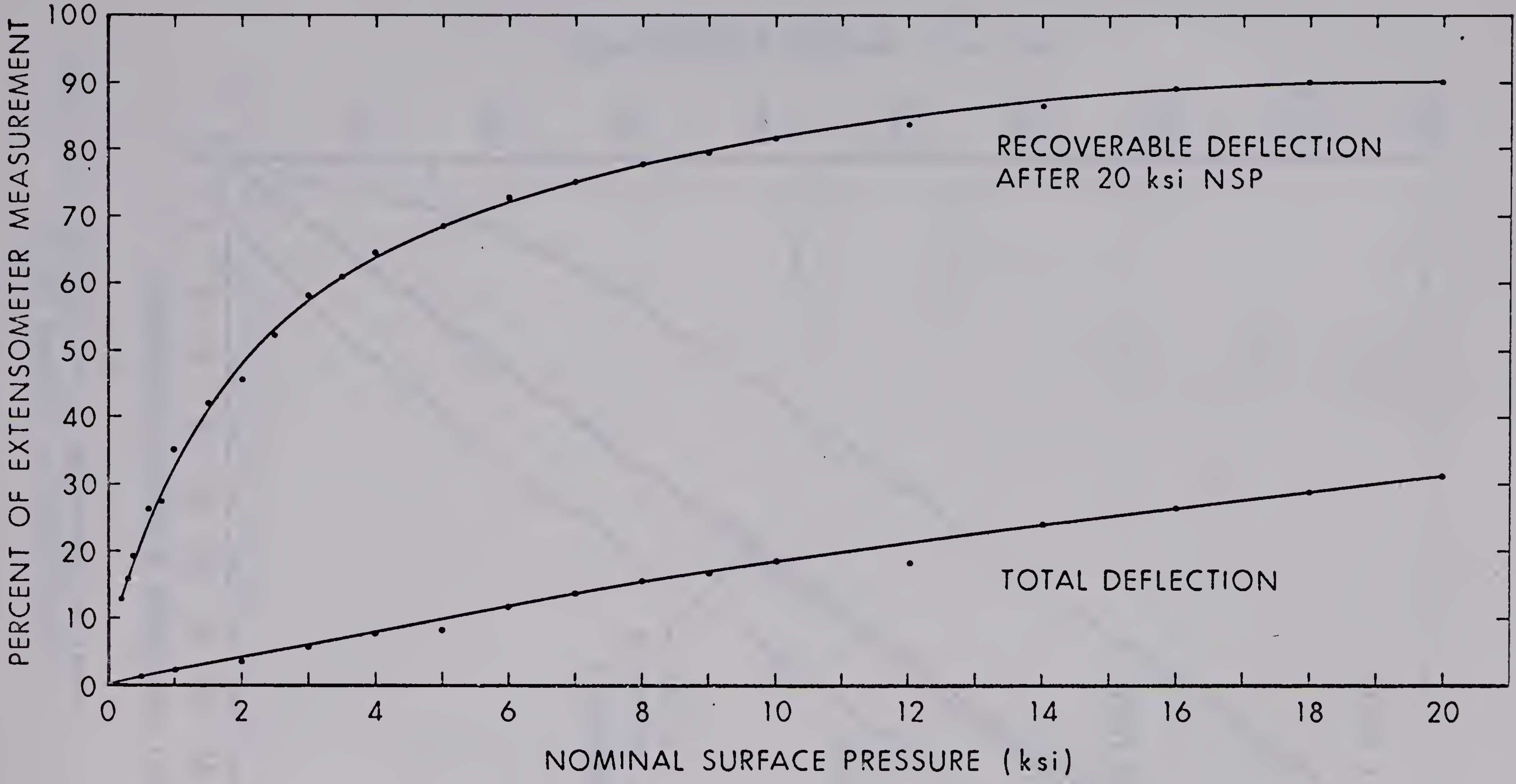

Figure 3-7 Strain Gauge Deflection ($\varepsilon \ell$) as Percent of Extensometer Measurement, Test III

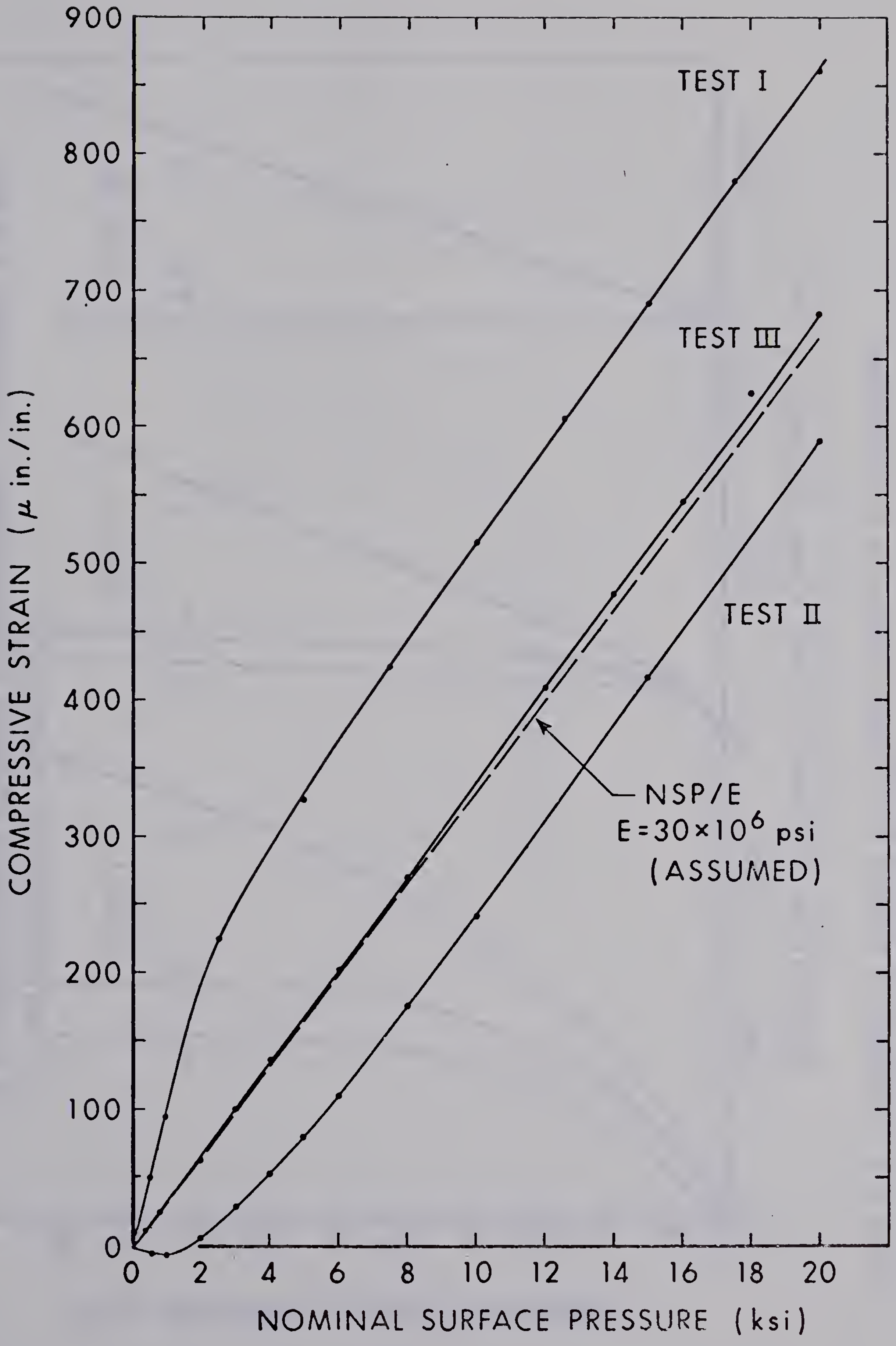

Figure 3-8 Average Strain Gauge Results after 20 ksi Nominal Surface Pressure

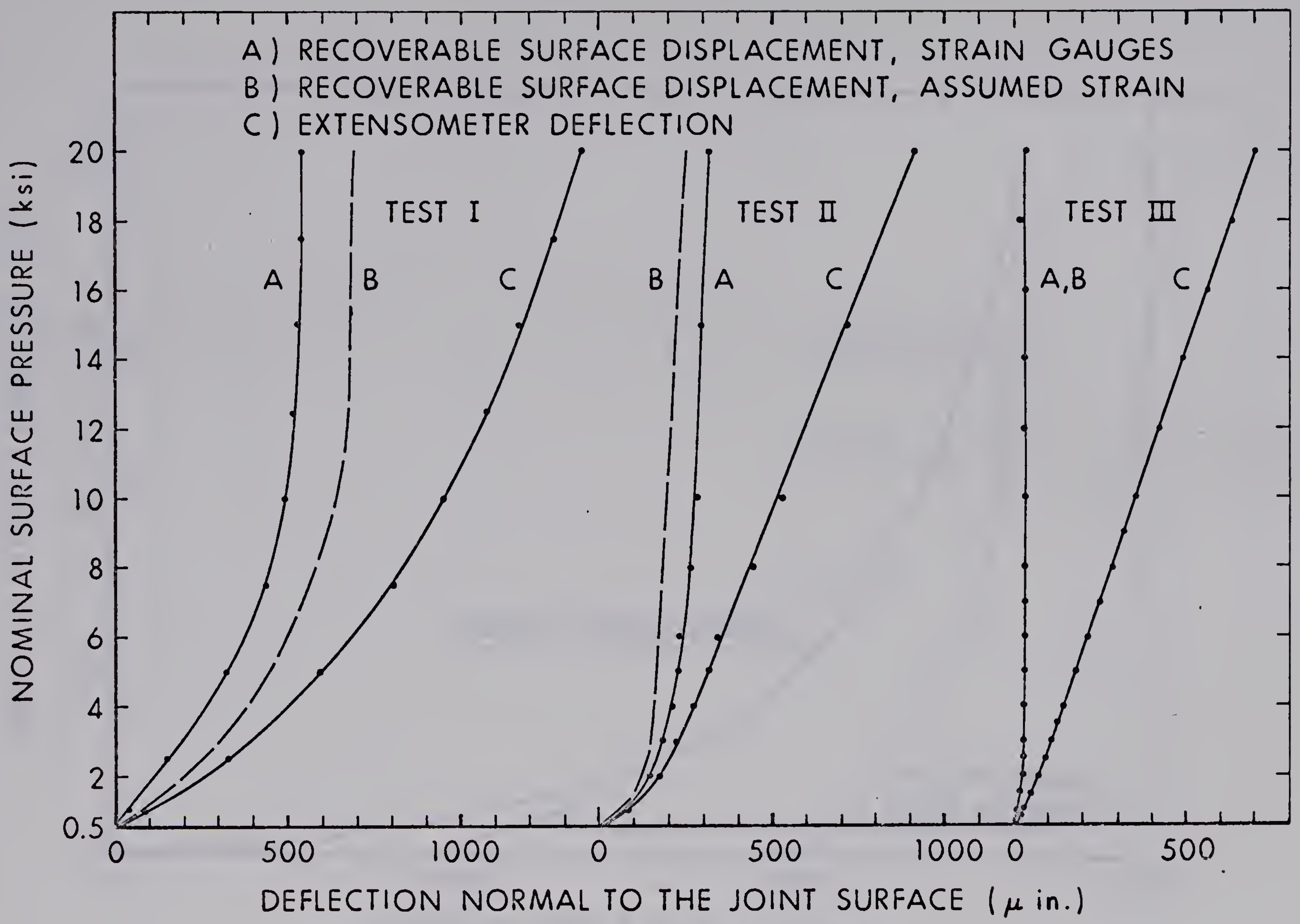

Figure 3-9 Recoverable Surface Displacement Based on Strain Gauge Results and Assumed Strain

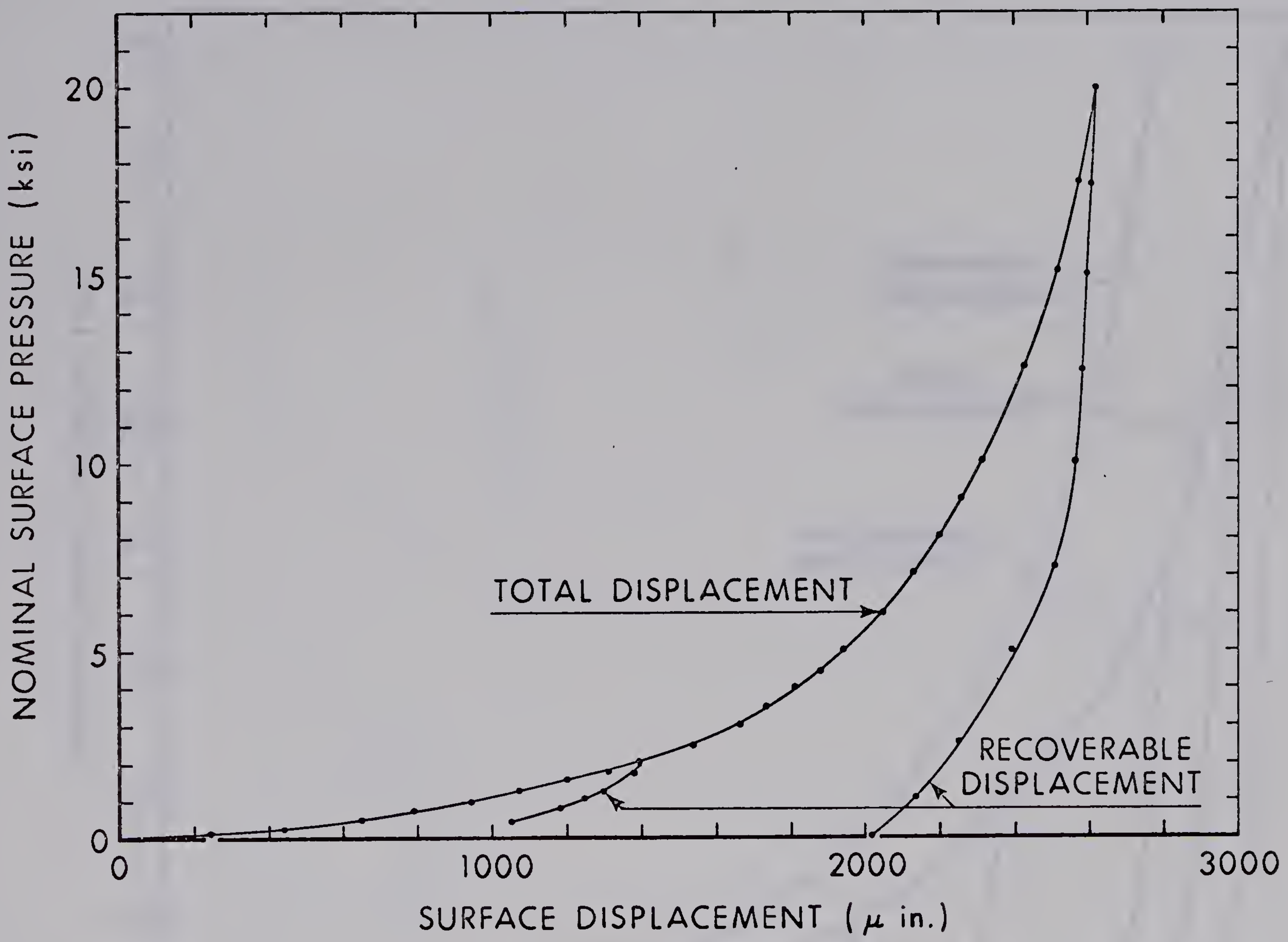

Figure 3-10 Loading Envelope, Test I

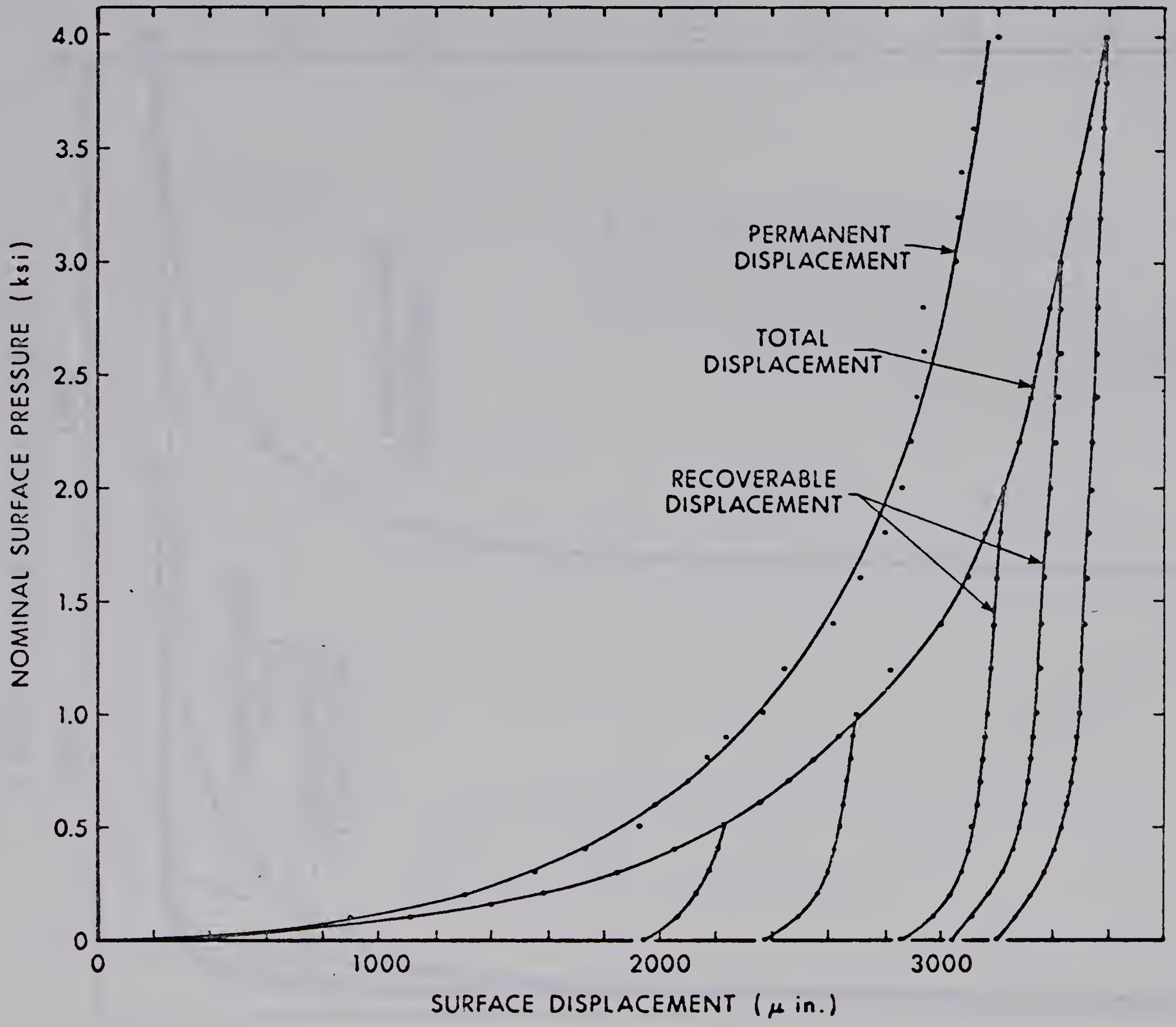

Figure 3-11 Loading Envelope, Test II

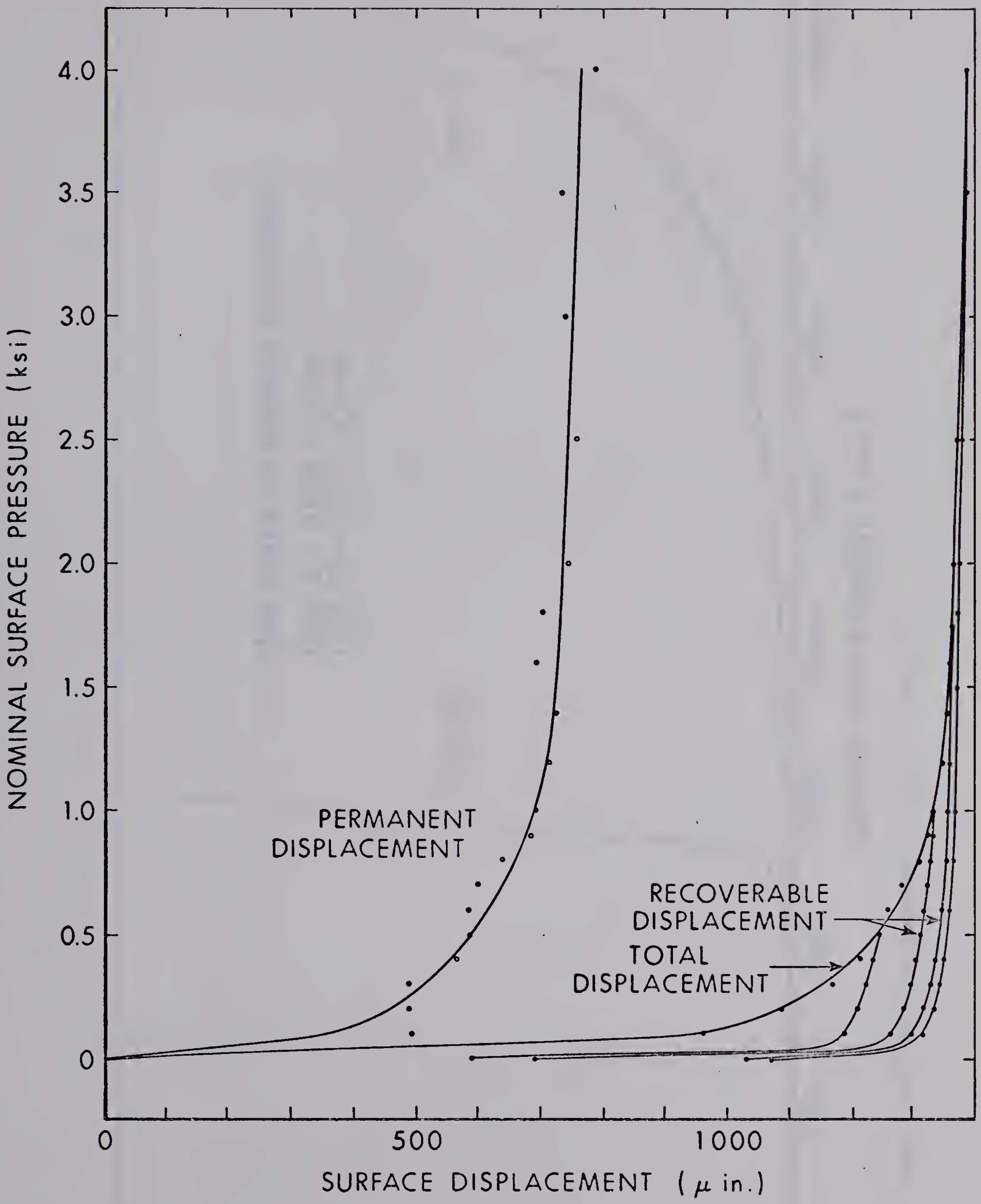

Figure 3-12 Loading Envelope, Test III

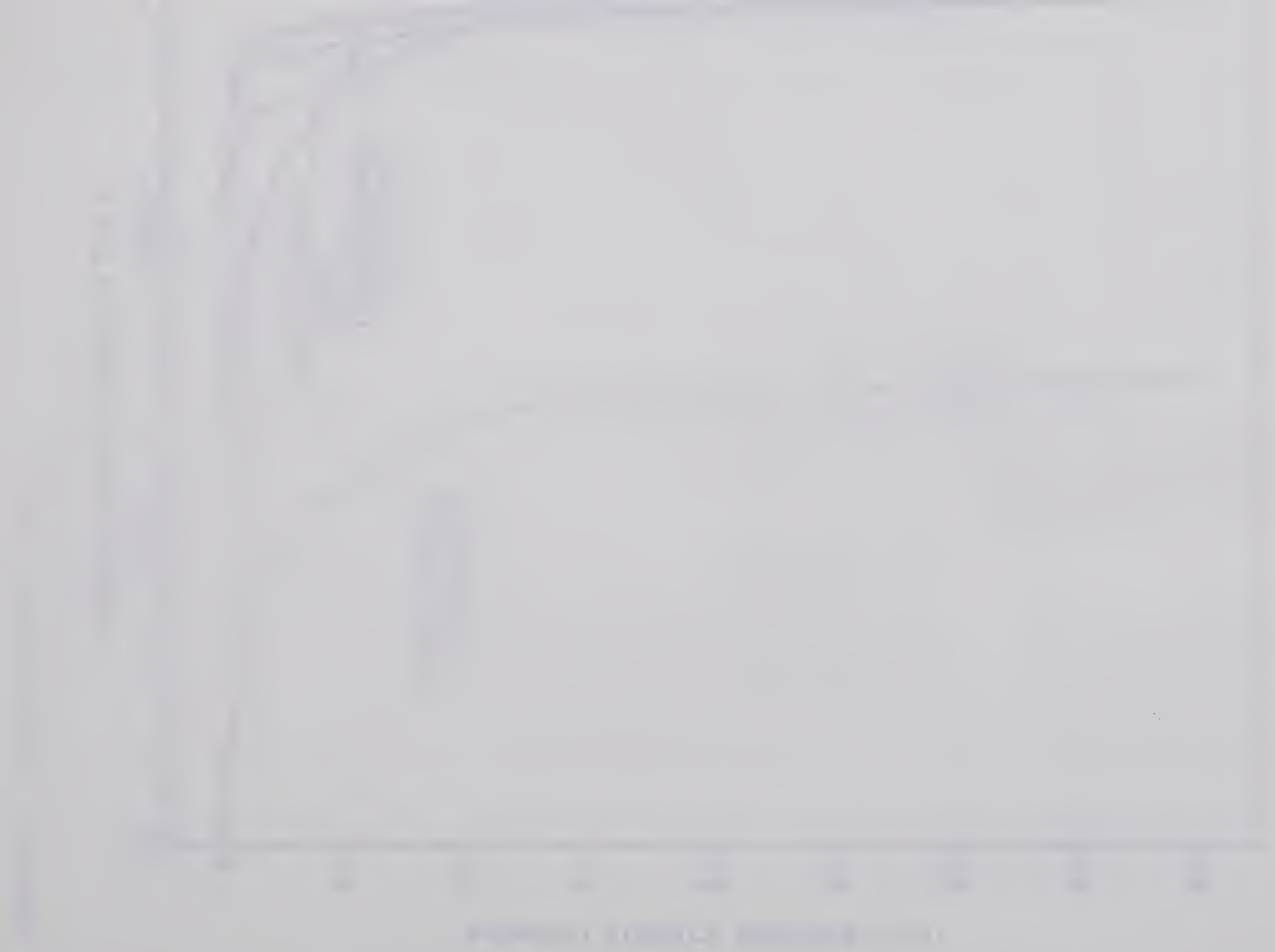

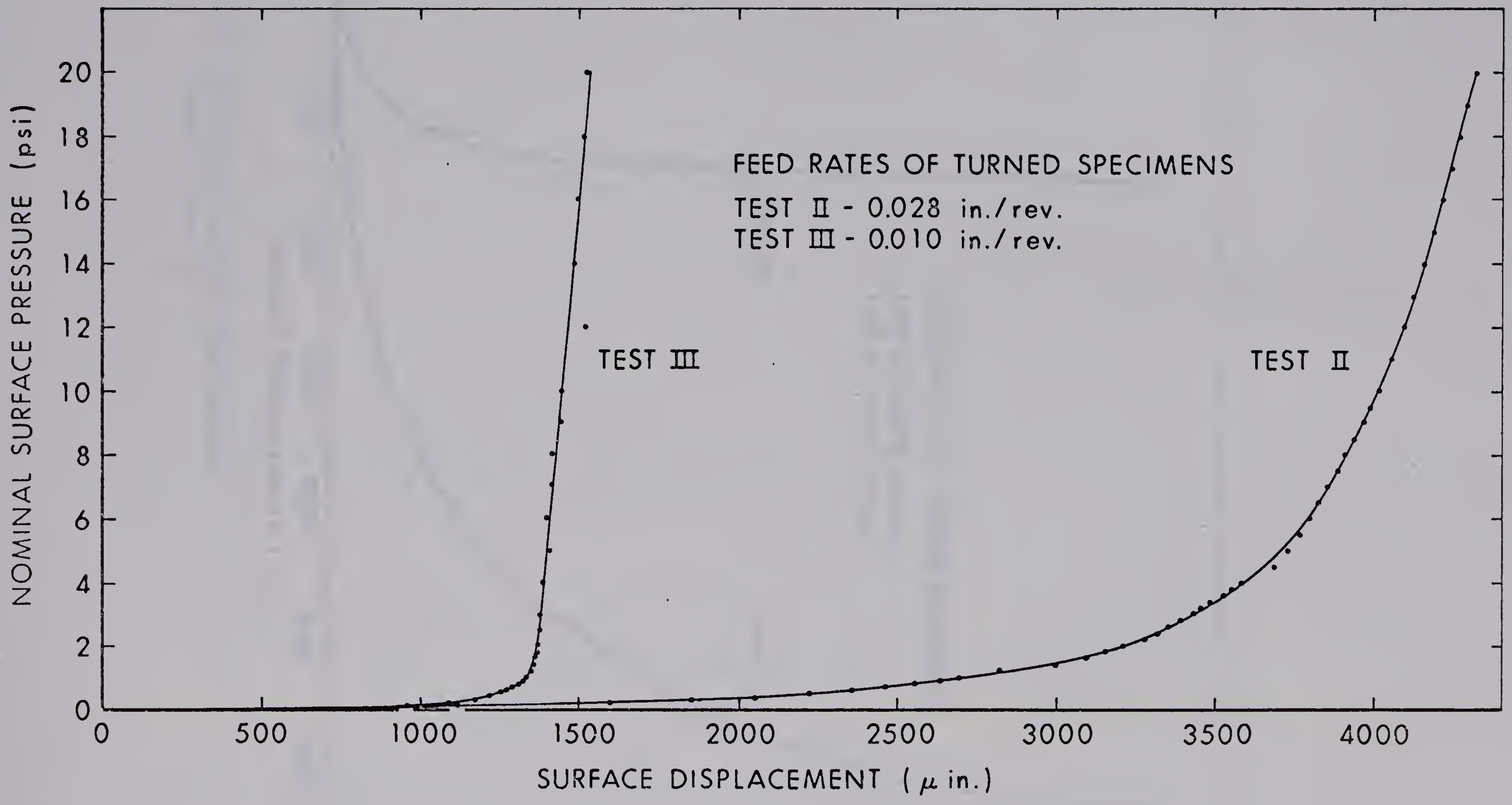

Figure 3-13 Total Surface Displacement, Tests II and III

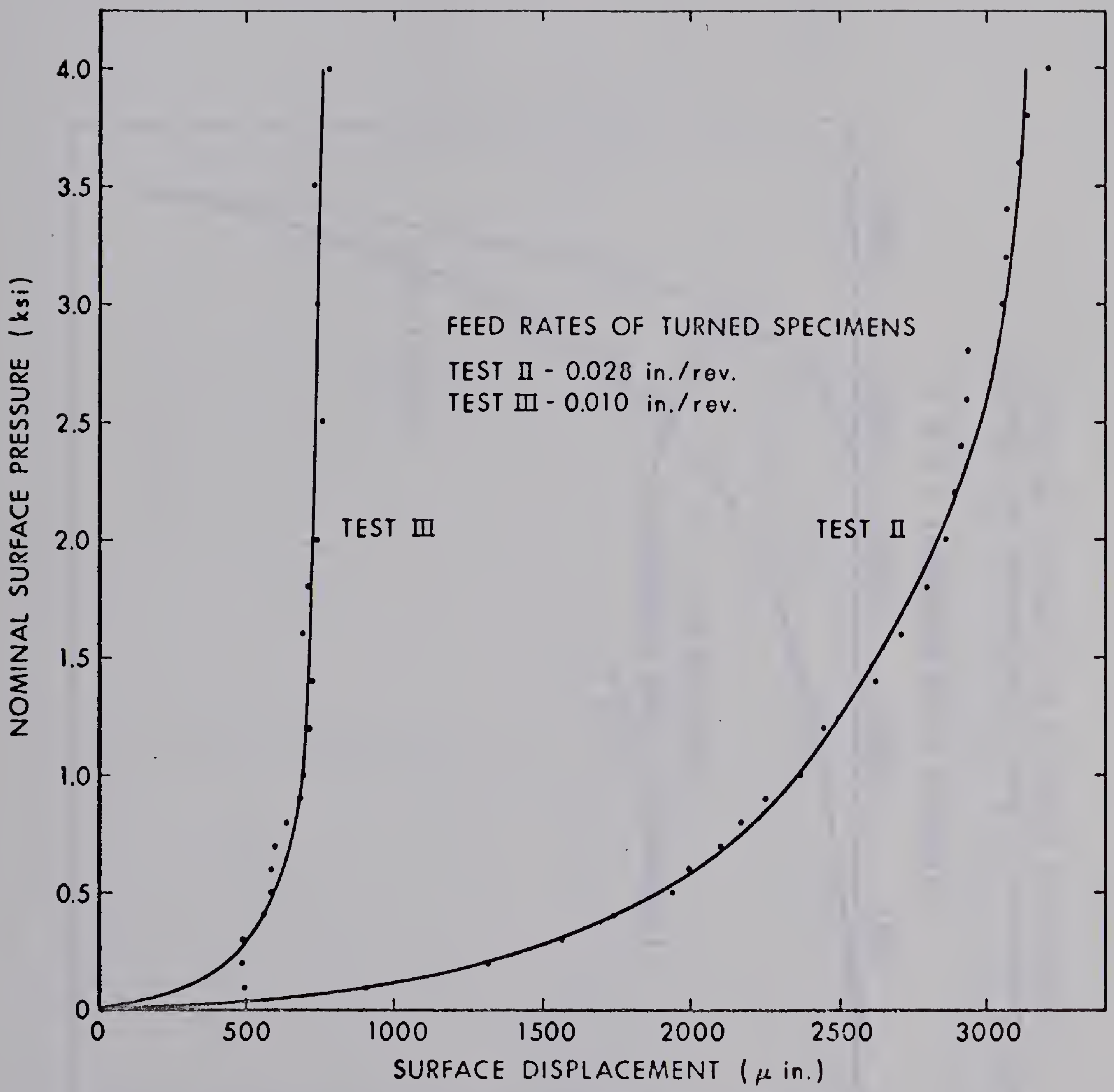

Figure 3-14 Permanent Surface Displacement, Tests II and III

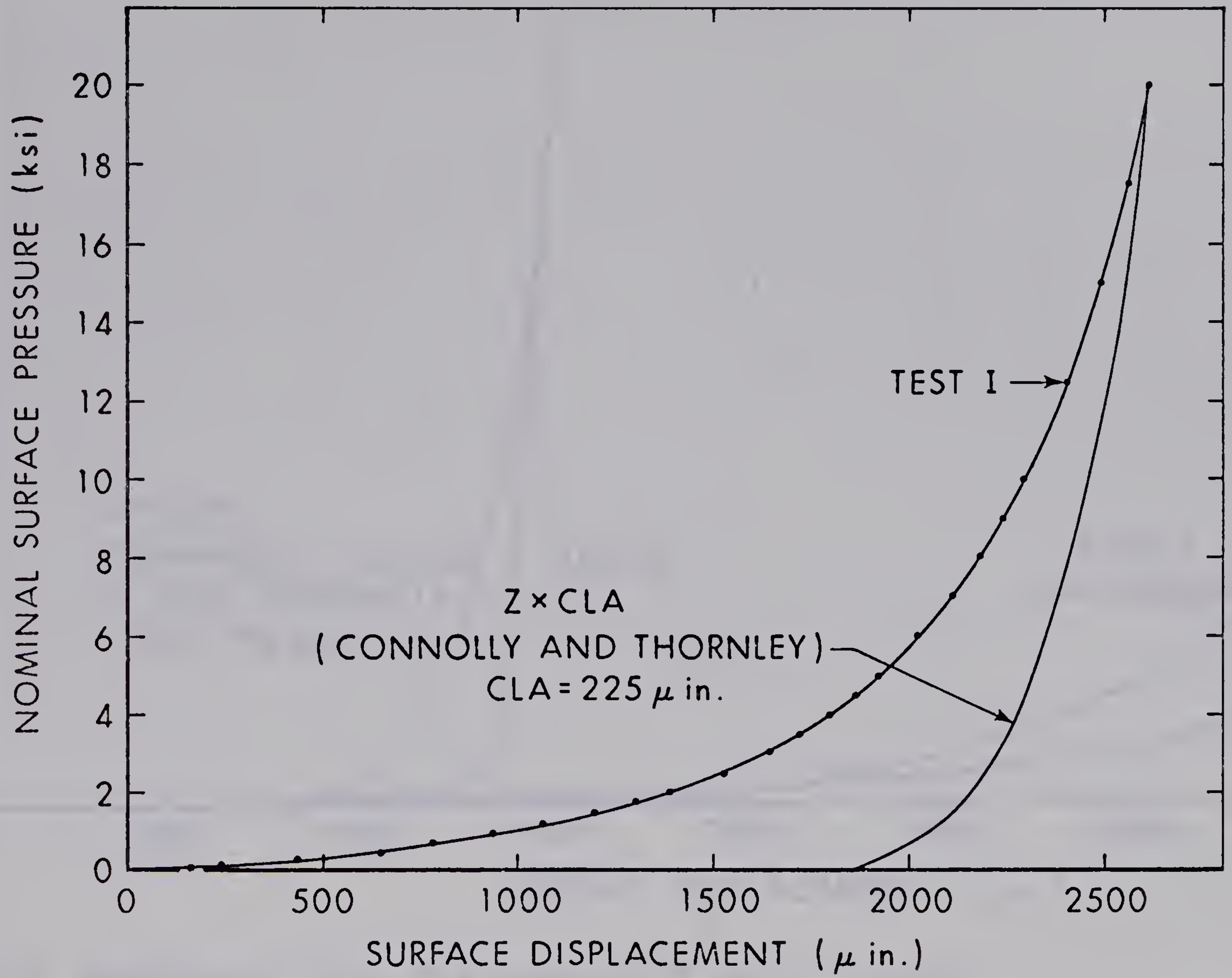

Figure 3-15 Comparison of Total Displacement with Results Obtained by Connolly and Thornley for Test I

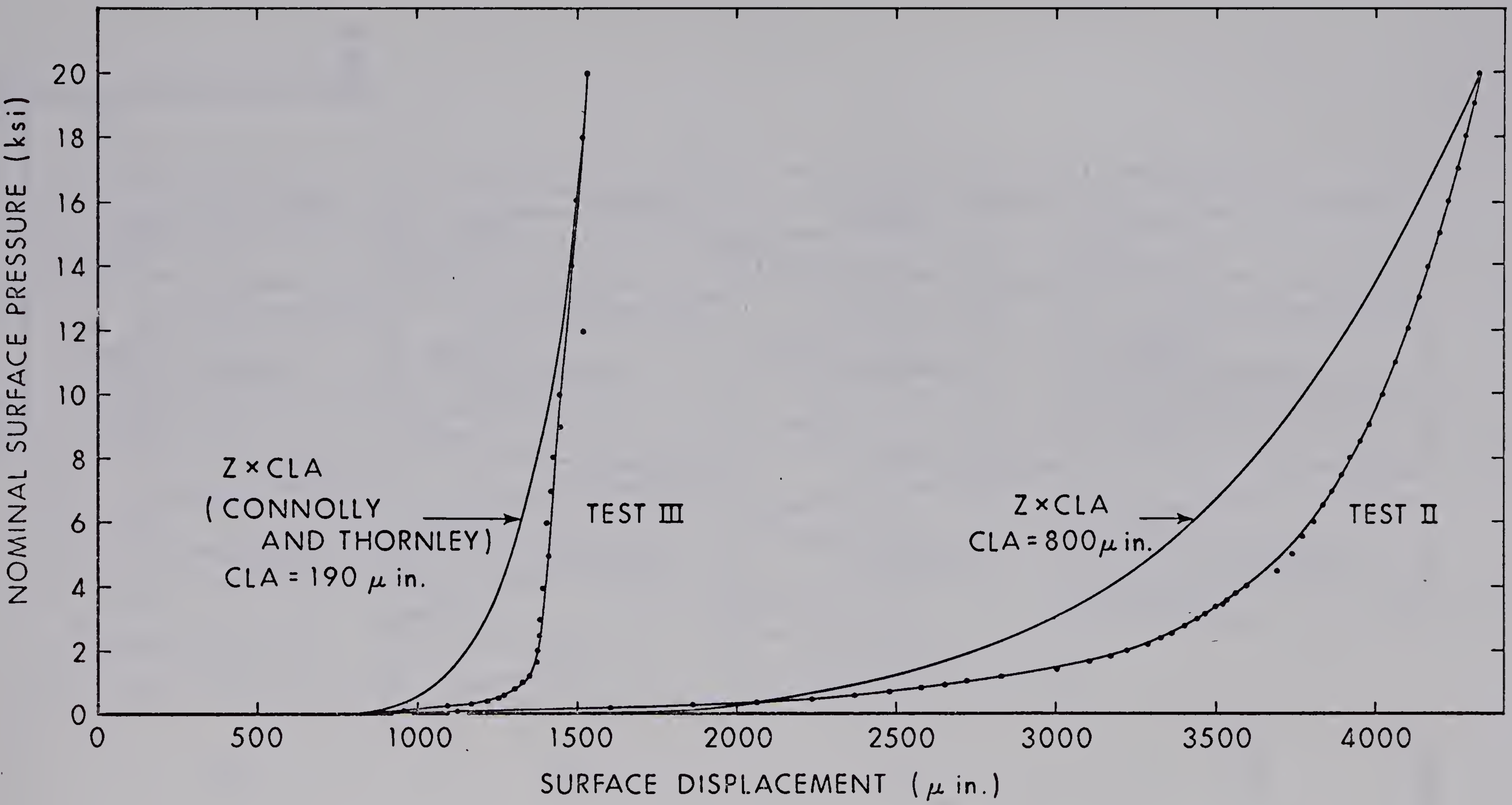

Figure 3-16 Comparison of Total Displacement with Results Obtained by Connolly and Thornley for Tests II and III

[illegible]

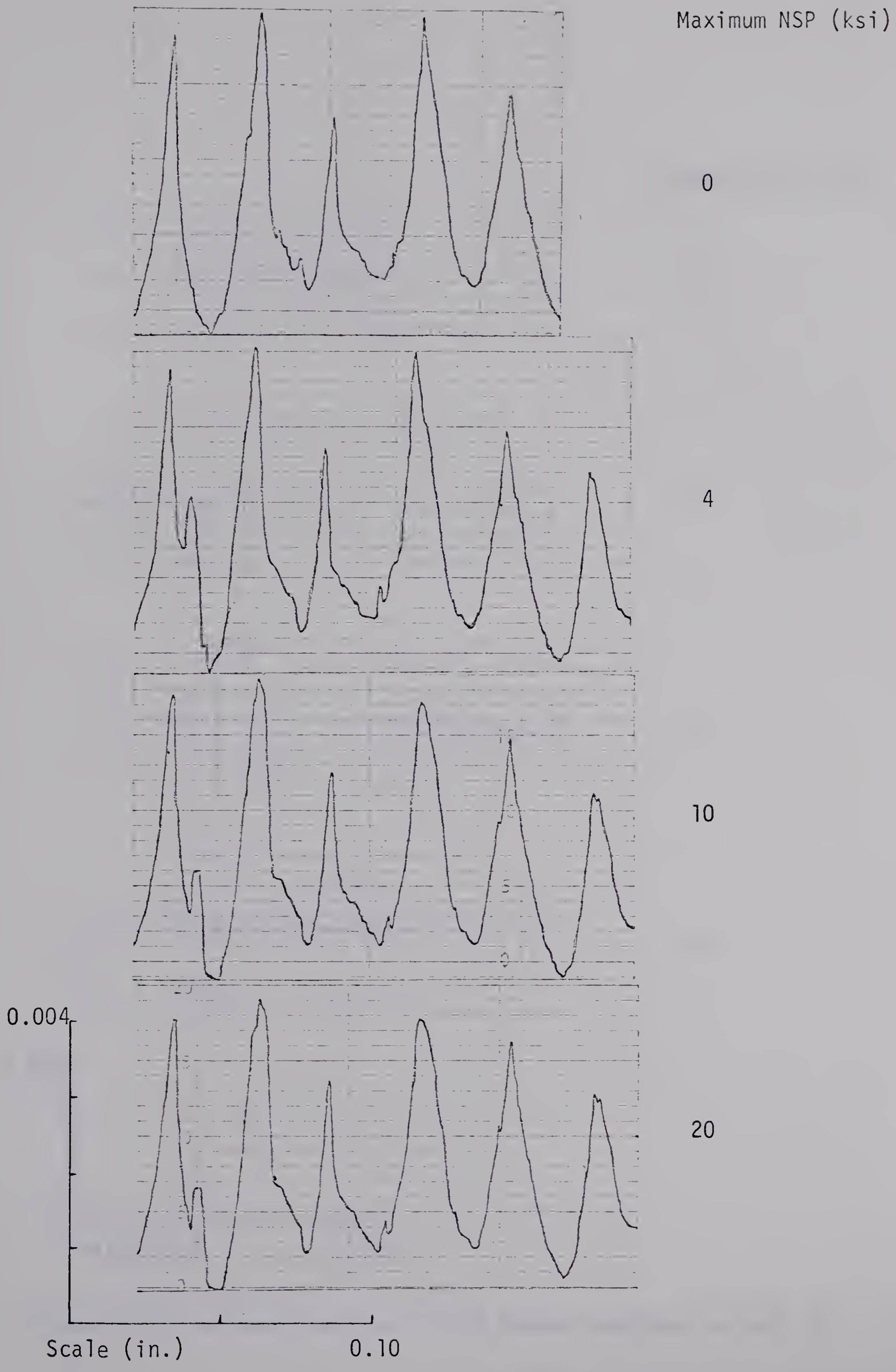

Figure 3-17 Surface Profiles of the Turned Specimen in Test II

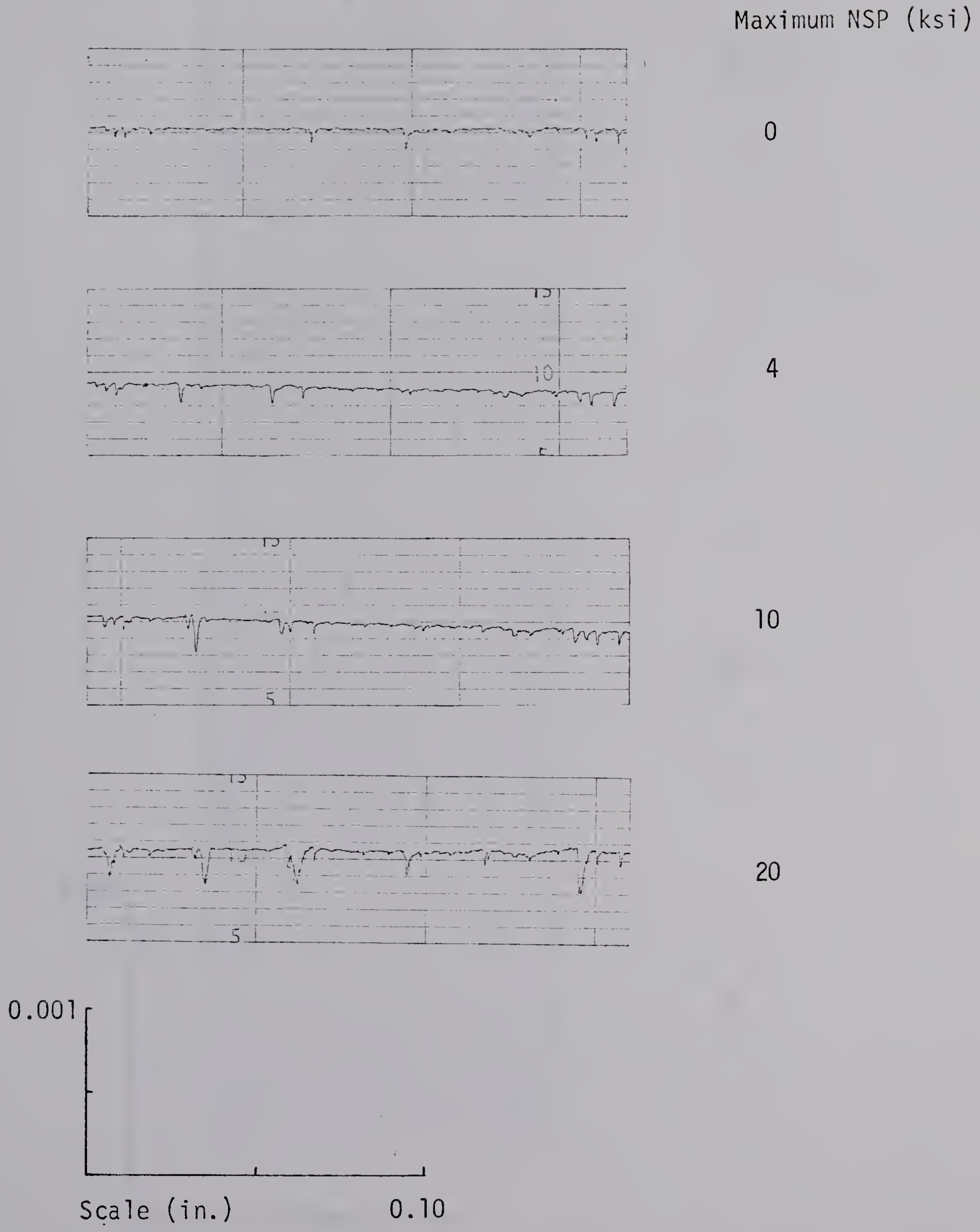

Figure 3-18 Surface Profiles of the Ground Specimen in Test II

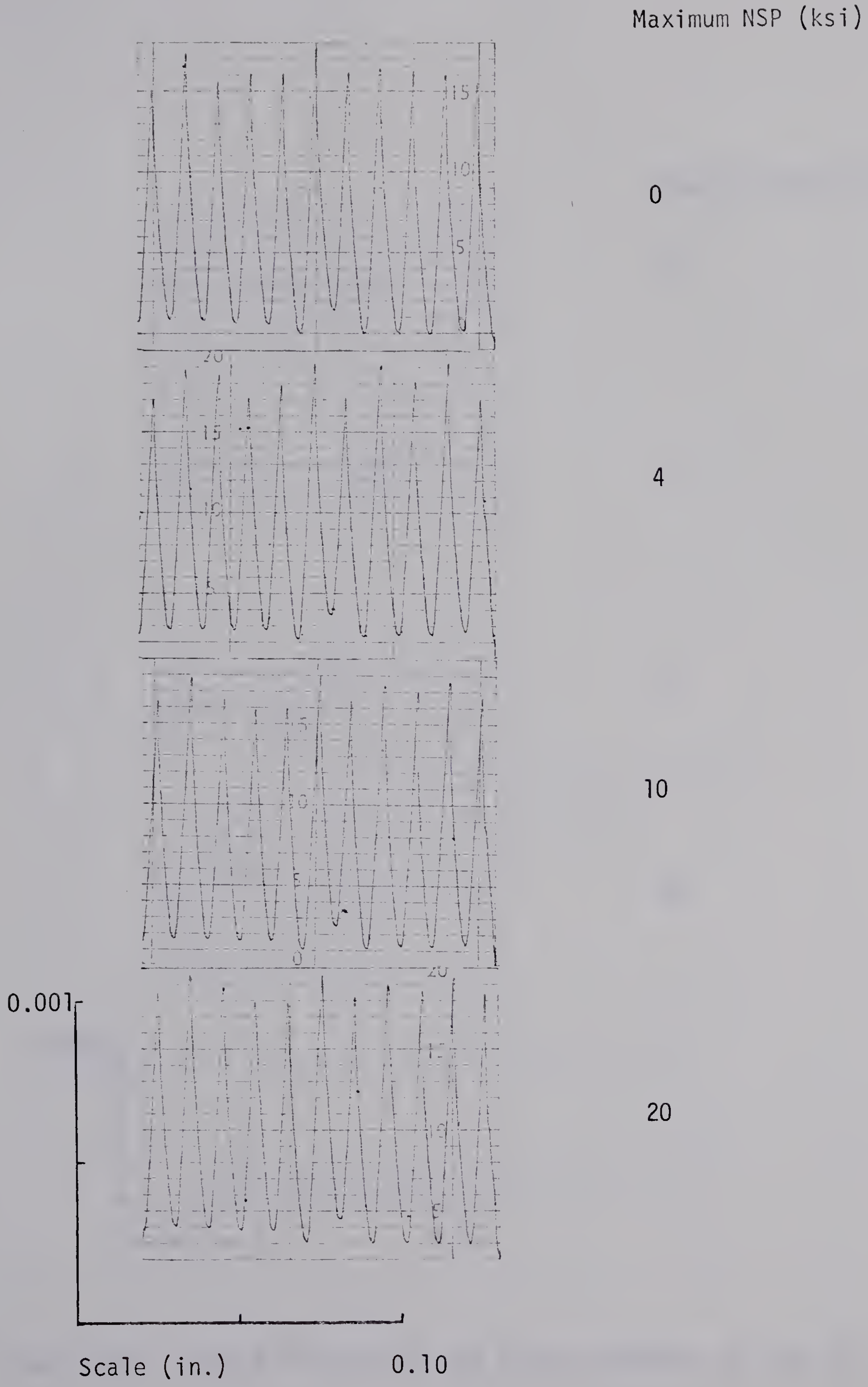

Figure 3-19 Surface Profiles of the Turned Specimen in Test III

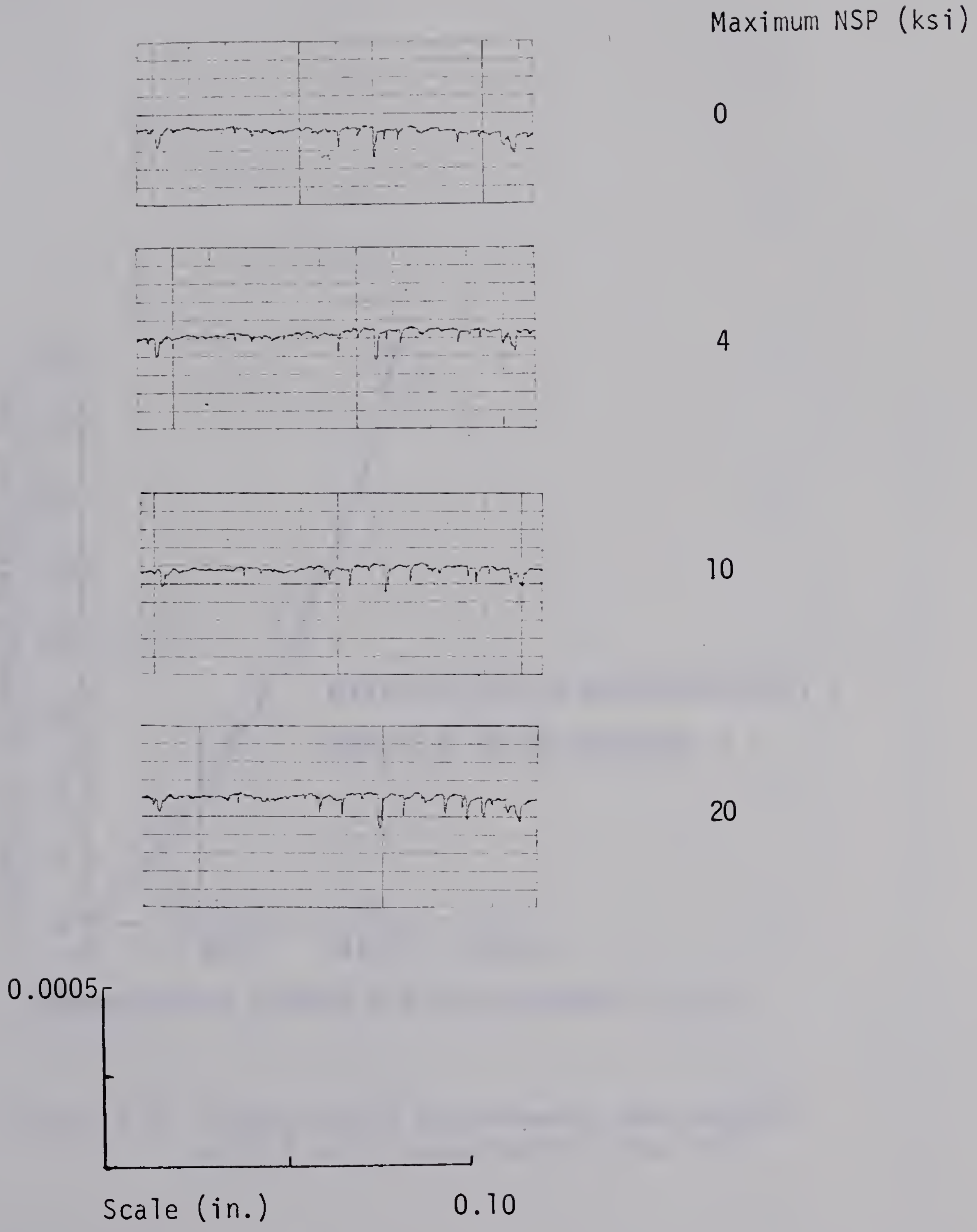

Figure 3-20 Surface Profiles of the Ground Specimen in Test III

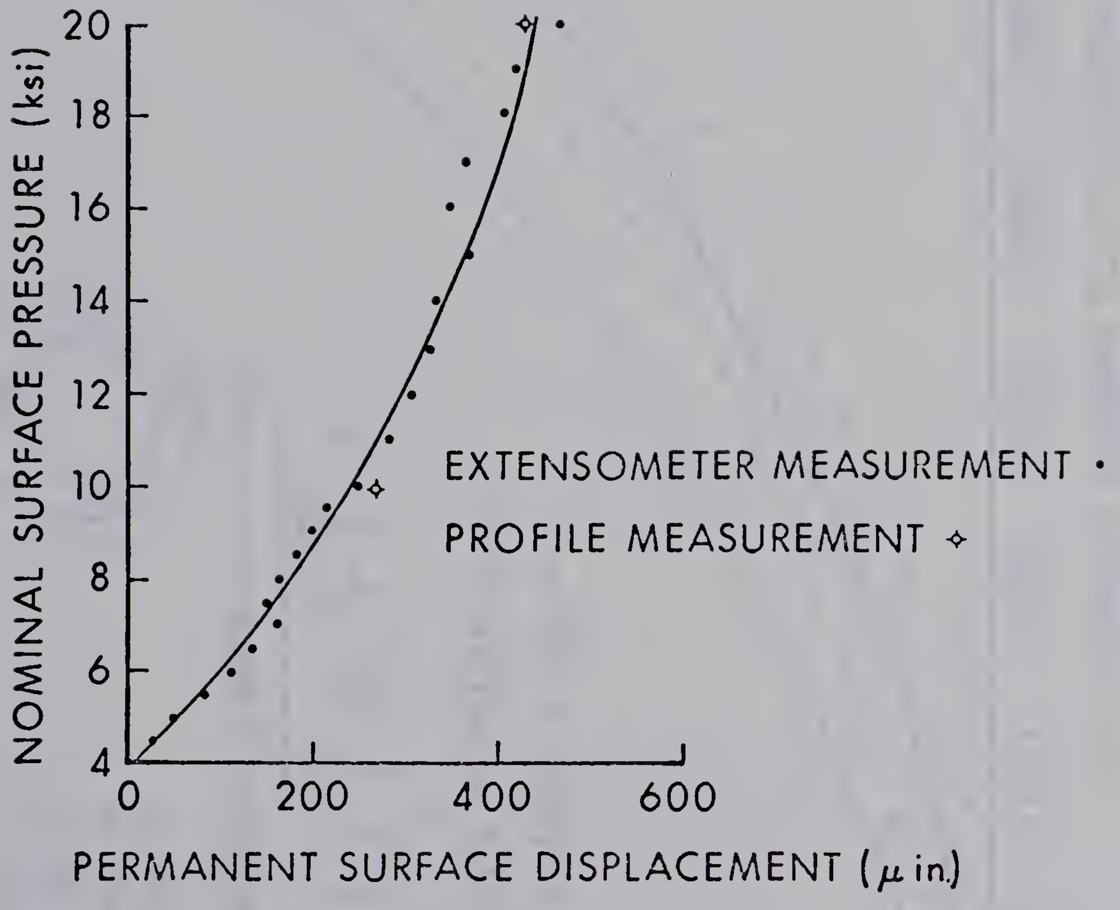

Figure 3-21 Comparison of Extensometer Measurements with Profile Measurements, Test II

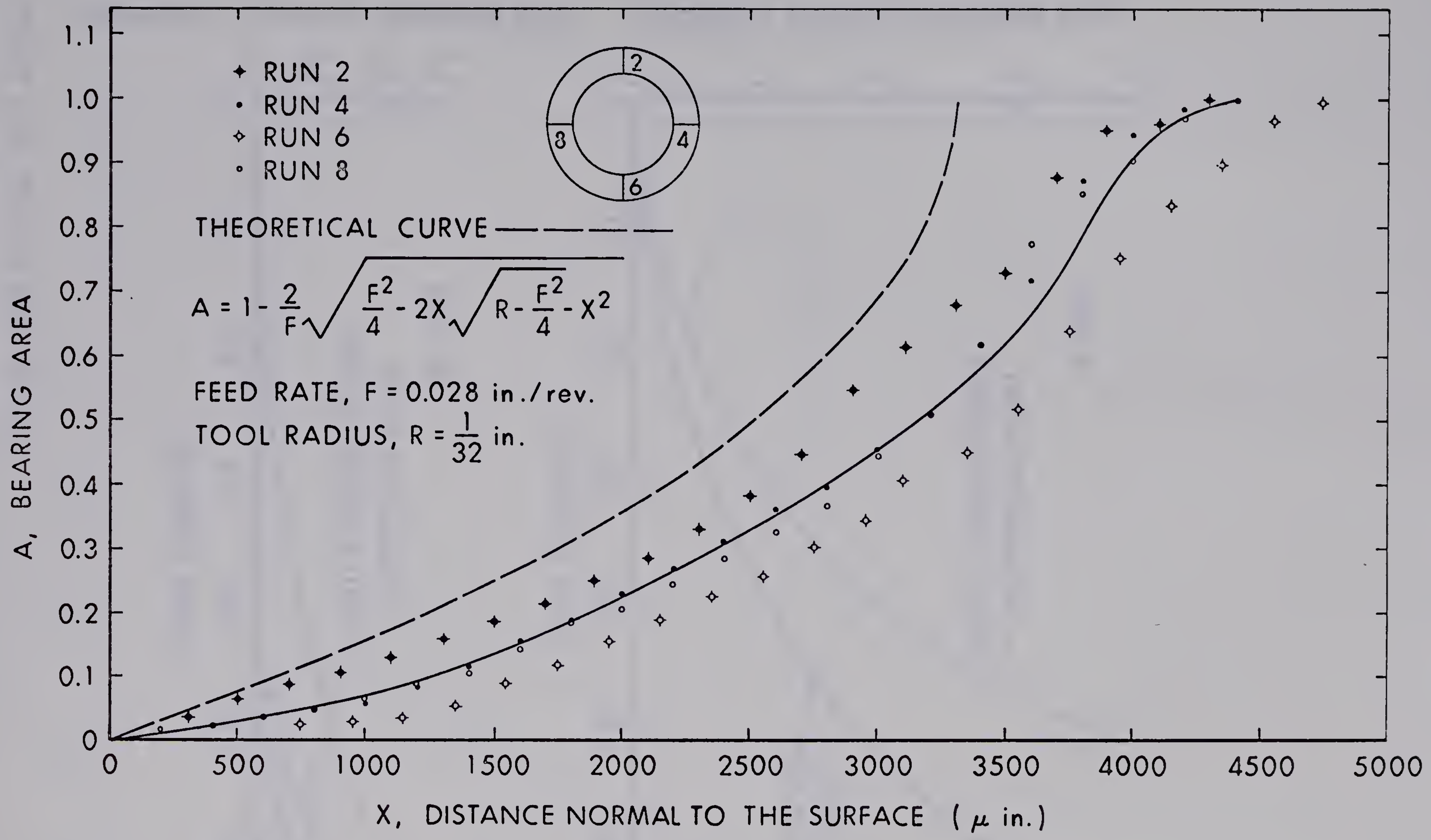

Figure 3-22 Bearing Area for the Turned Specimen in Test II

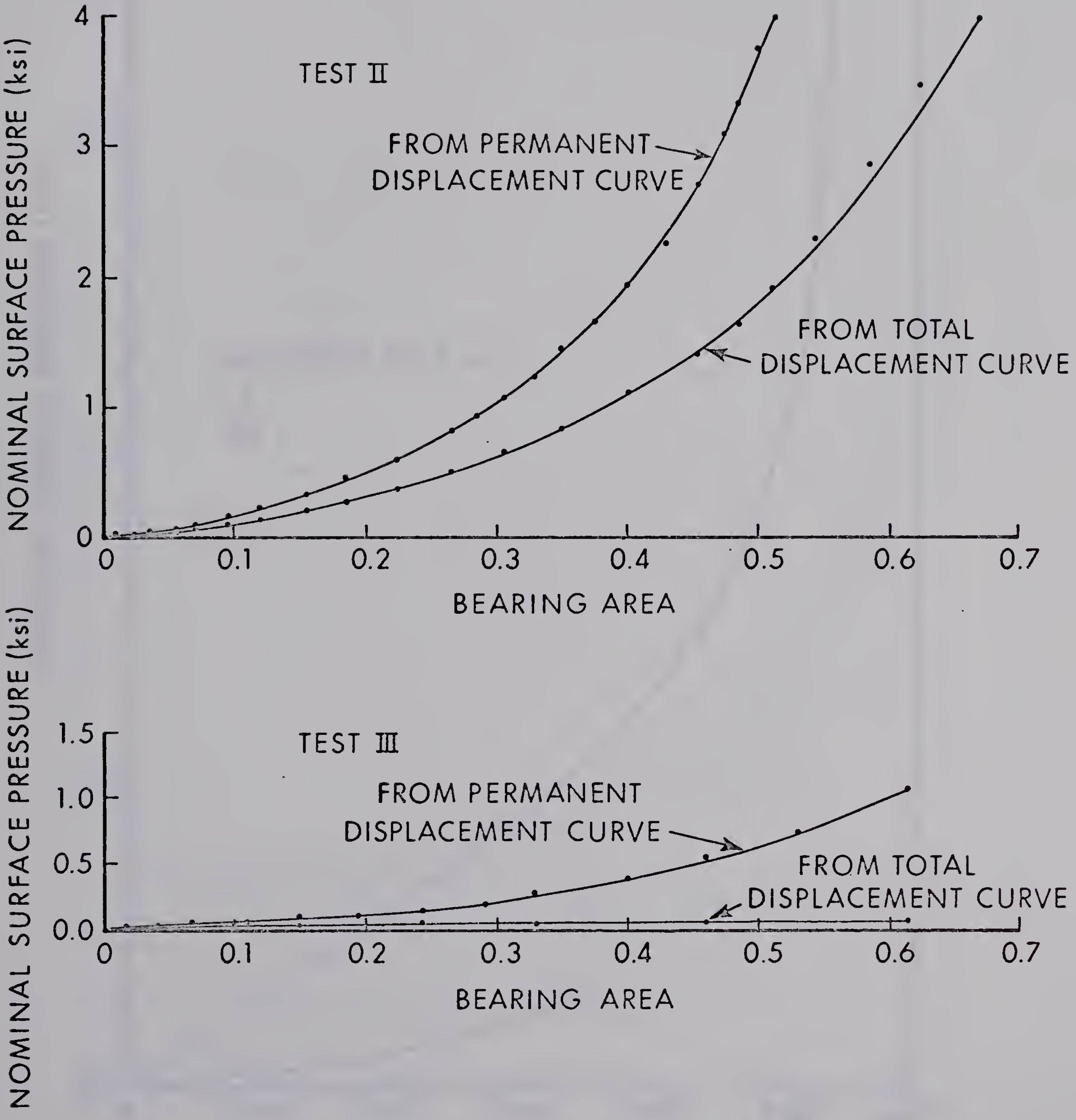

Figure 3-23 Bearing Area Results

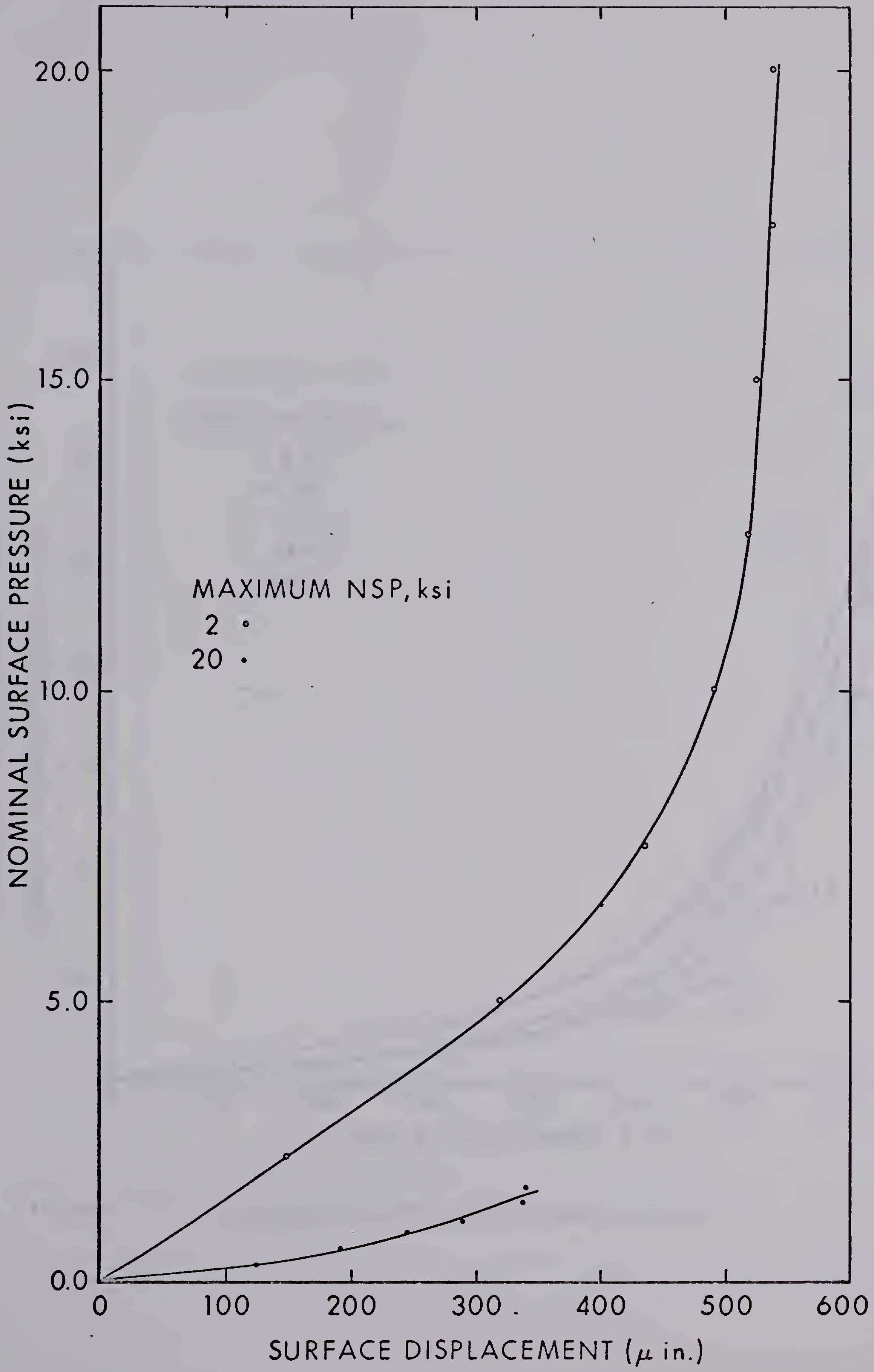

Figure 3-24 Recoverable Surface Displacement, Test I

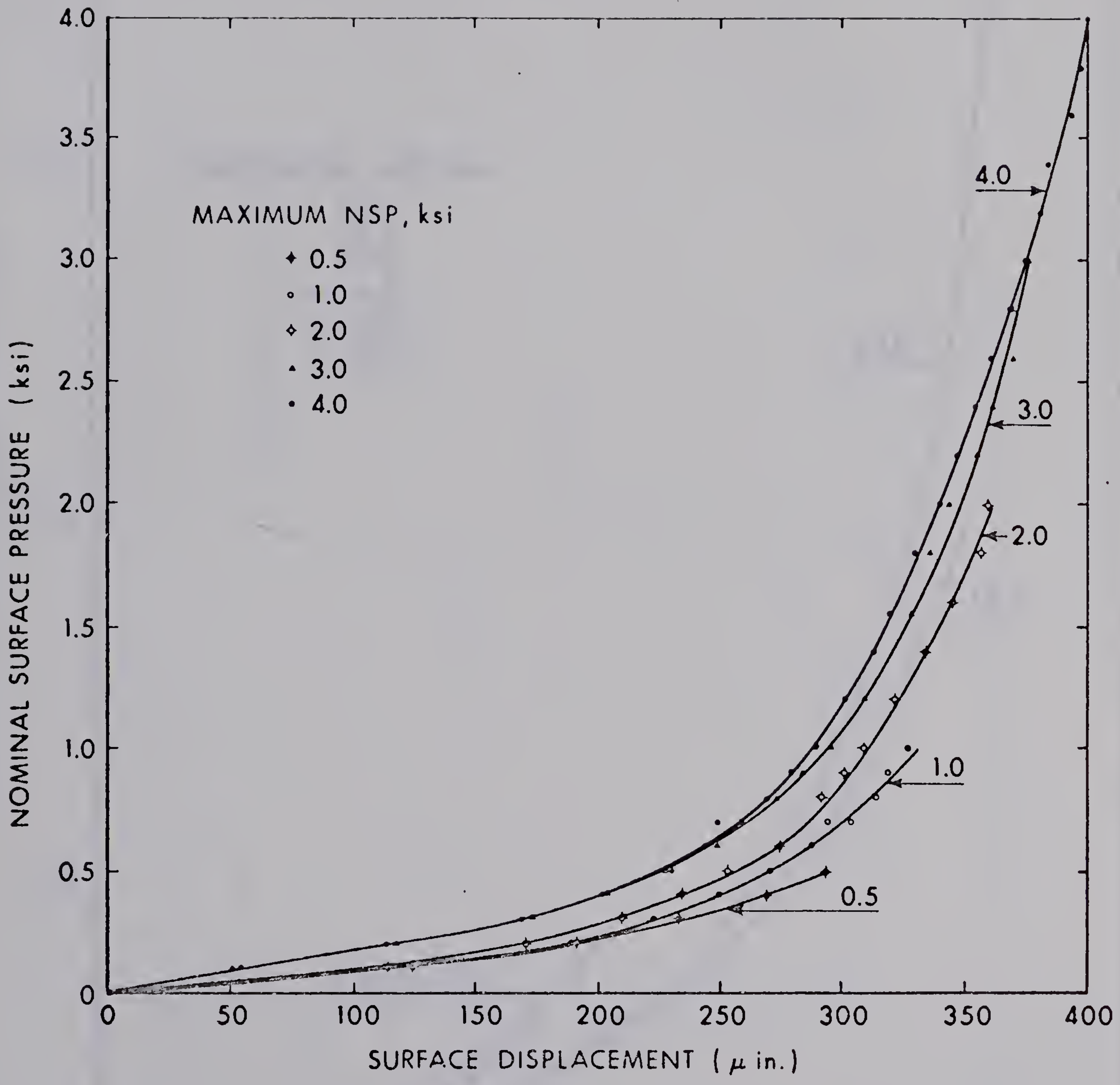

Figure 3-25 Recoverable Surface Displacement, Test II

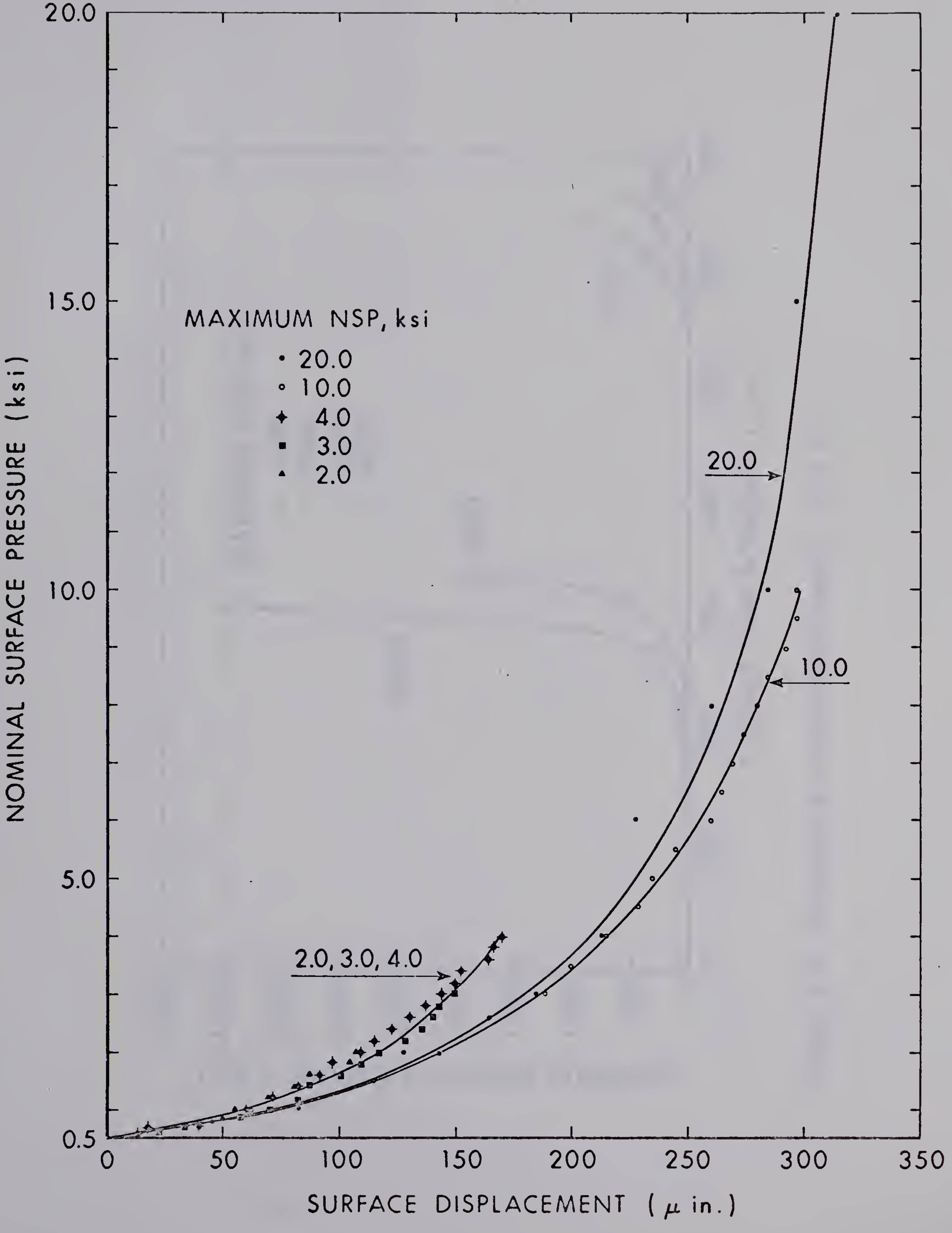

Figure 3-26 Recoverable Surface Displacement, Test II

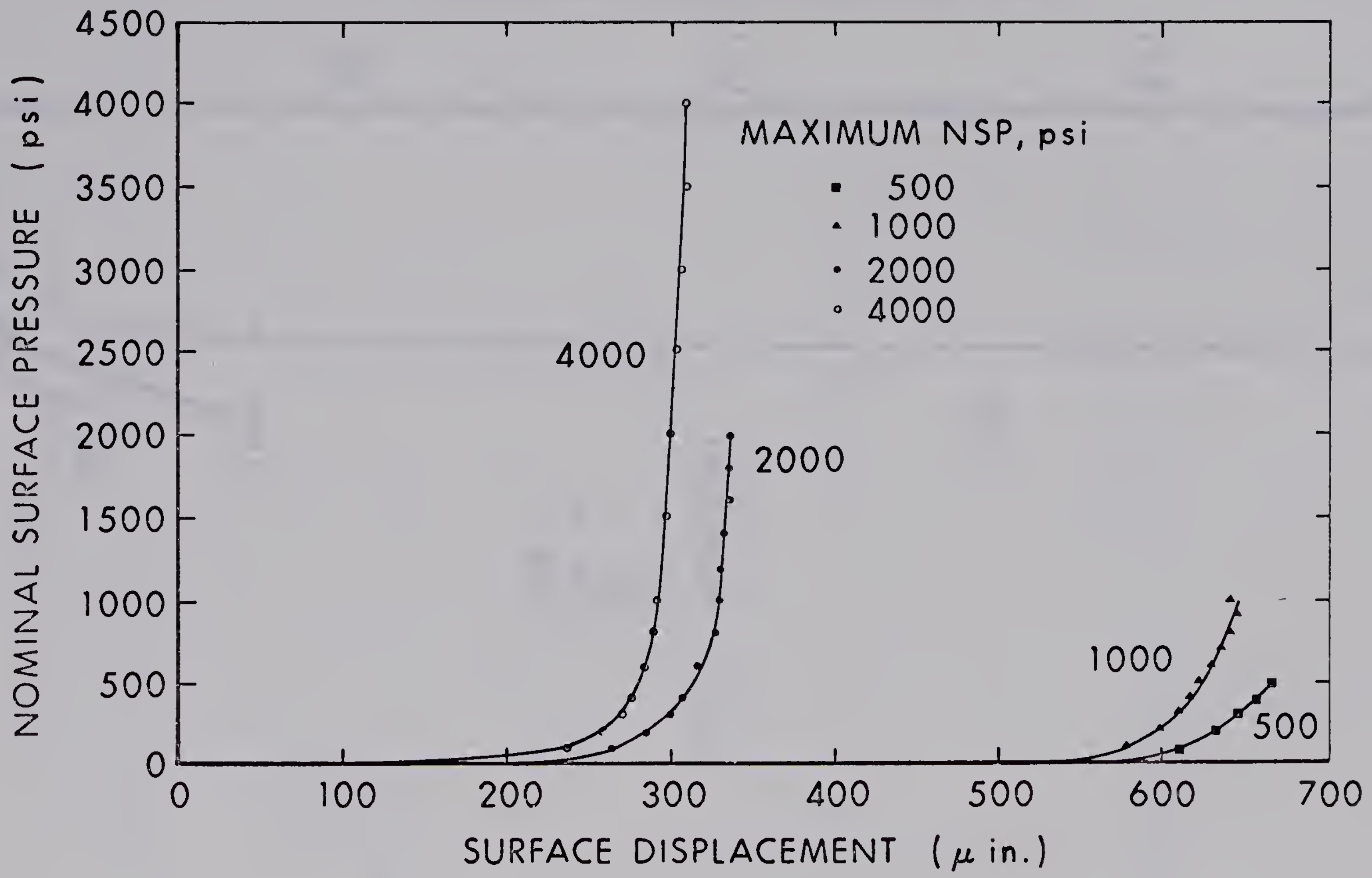

Figure 3-27 Recoverable Surface Displacement, Test III

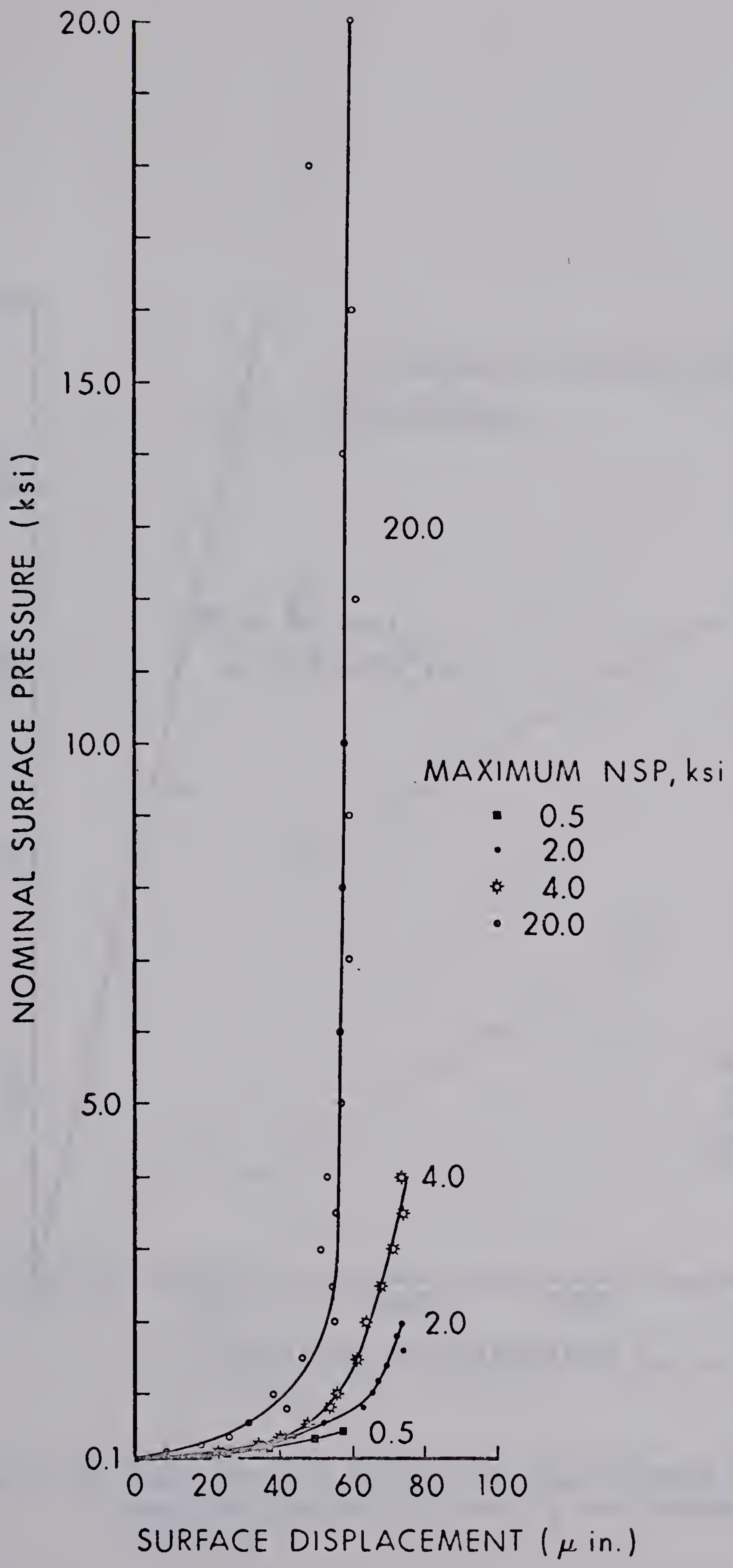

Figure 3-28 Recoverable Surface Displacement, Test III

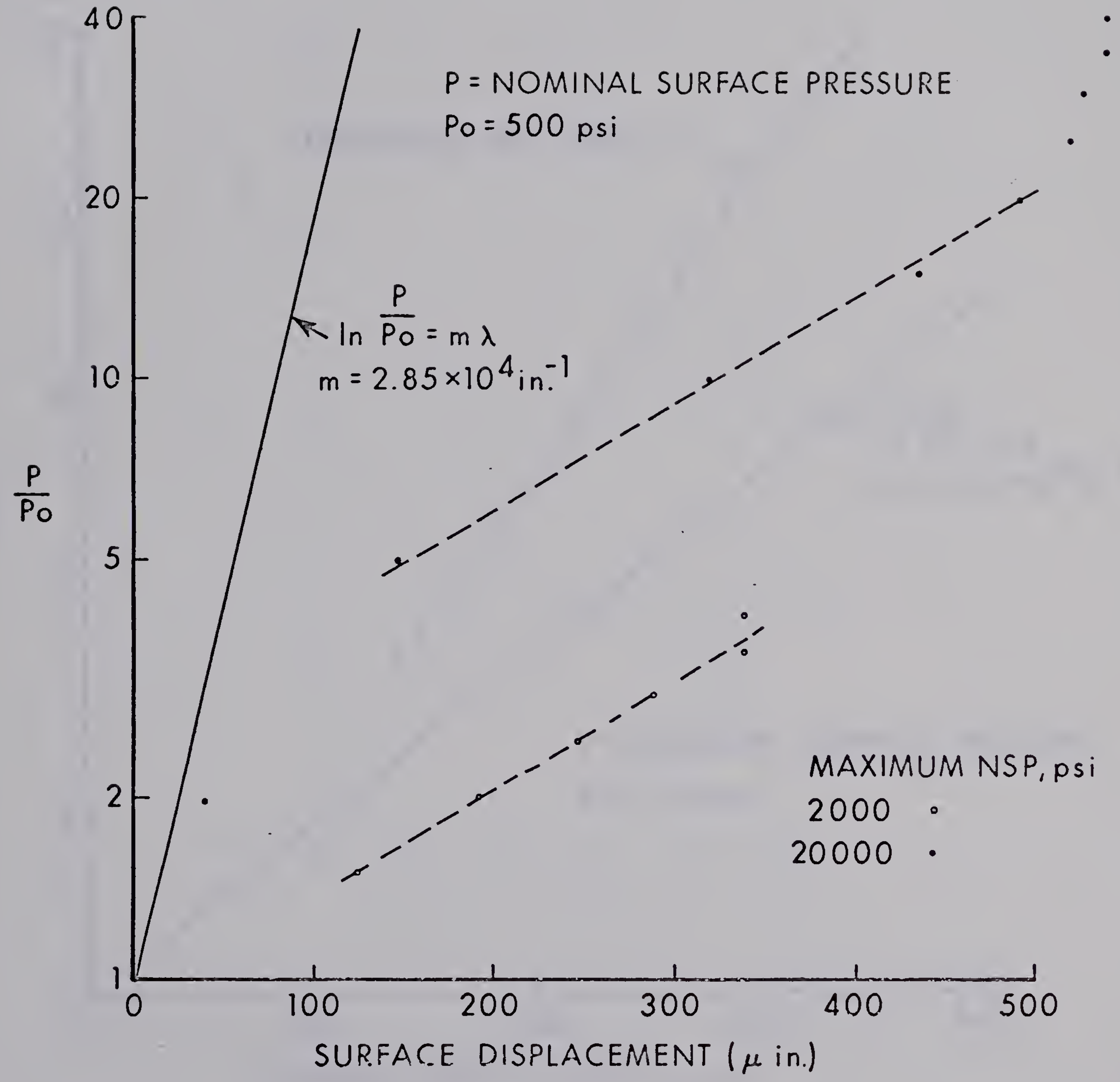

Figure 3-29 Comparison of Recoverable Displacement With Results Obtained by Connolly and Thornley for Test I

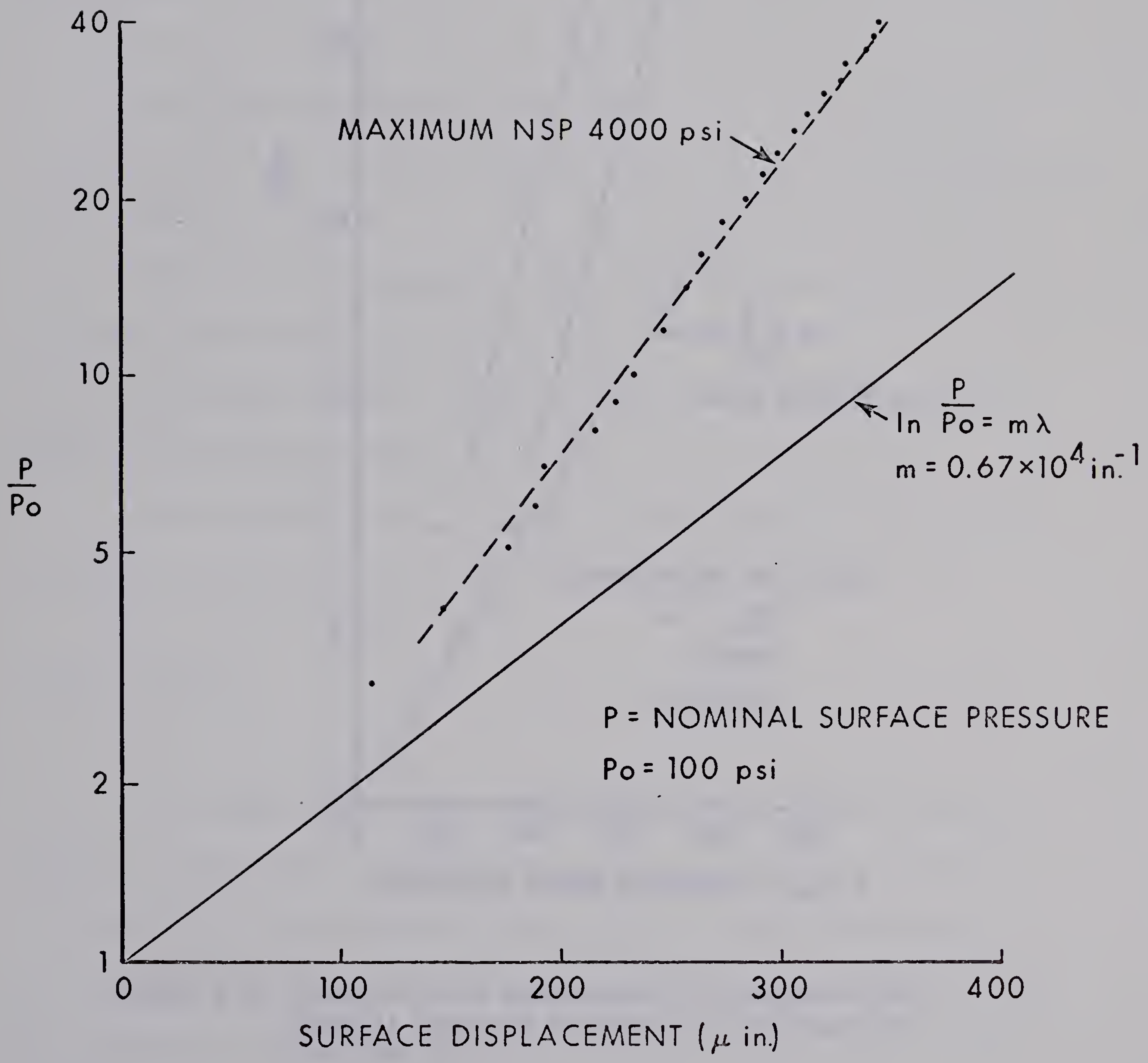

Figure 3-30 Comparison of Recoverable Displacement With Results Obtained by Connolly and Thornley for Test II

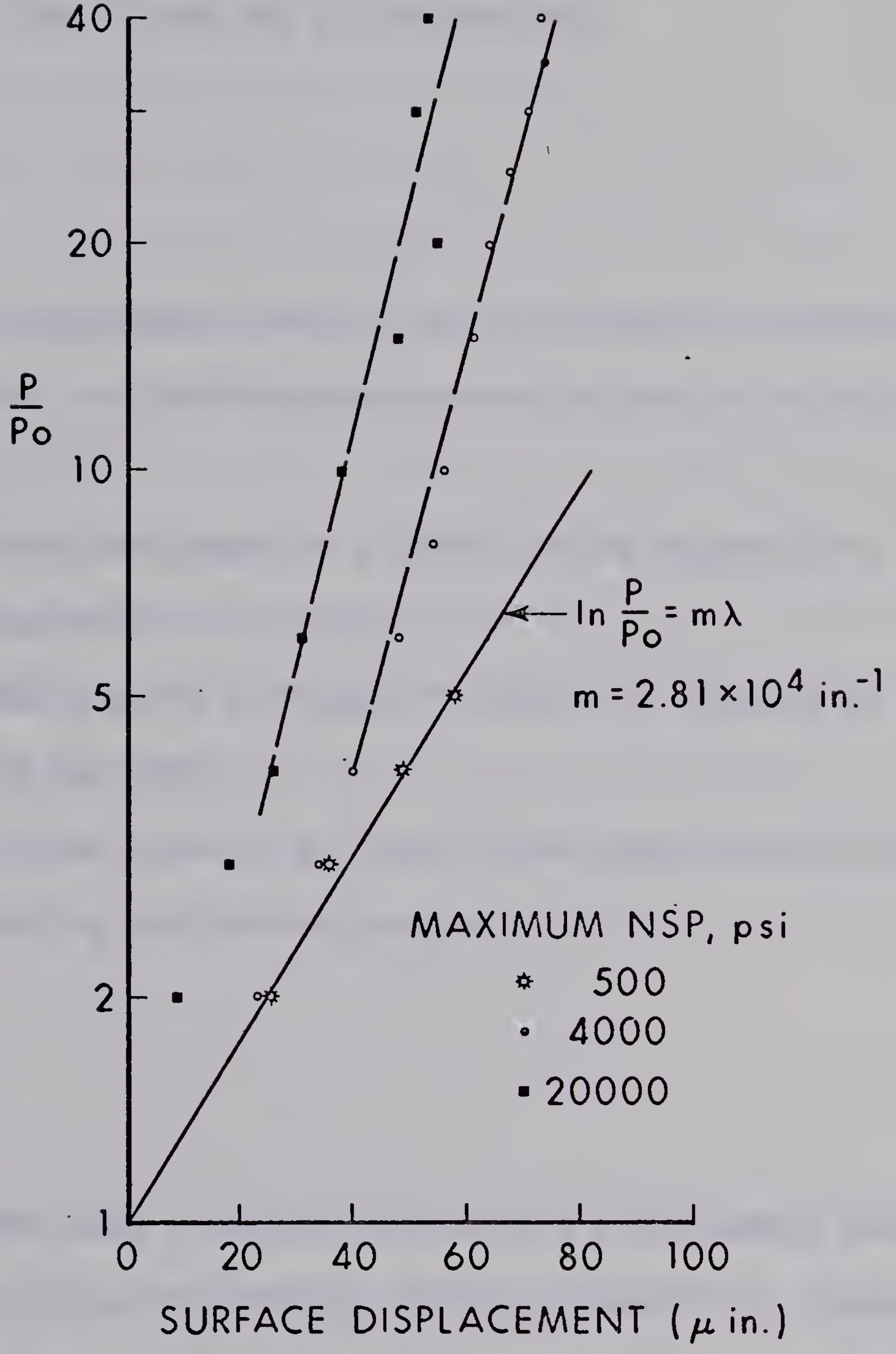

Figure 3-31 Comparison of Recoverable Displacement With Results Obtained by Connolly and Thornley for Test III

CHAPTER IV

CONCLUSIONS AND RECOMMENDATIONS

Conclusions

1. Surface displacement results can be affected by assuming the compressive strain in a joint specimen to be the same as in an equivalent solid component.
2. The surface topography of a joint surface changes with an increase in the maximum normal load.
3. The normal elastic stiffness of a joint is affected by the loading history of the joint.
4. The CLA value alone is an insufficient description of surface texture for predicting surface displacement.

Recommendations

1. The method used in determining surface displacement could be applied to other joints of different shapes and materials. However, for loading joint specimens on a testing machine, the minimum load should be applied with a dead weight attached to the top joint specimen. The accuracy of the minimum load would then be constant for all load ranges.
2. A more conclusive relationship between changes in surface profile and permanent surface displacement could probably be achieved by reducing the total number of asperities on the contact surface of

a joint specimen. This could be done by reducing the cross sectional area of the contact surfaces.

3. It is now desirable to determine the type of joints whose elastic stiffness is most sensitive to an increase in maximum nominal surface pressure. In some cases it should be possible to simplify the machining process required to produce a joint of a given stiffness by applying a preload. Information concerning the effects of surface texture on the amplitude of a joint under dynamic normal load would also be valuable and could be the subject for further research.

4. Until design formulas are developed that incorporate factors other than specification of the machining operation and the CLA value, decisions on joint stiffness should be based on experiment.

REFERENCES

1. British Standard 1134, "Center Line Average Height Method for the Assessment of Surface Texture", British Standards Institution, 1961.
2. Kragelsky, I.V., and Demkin, N.B., "Contact Area of Rough Surfaces", Wear, Vol. 3, 1960, p. 170.
3. Abbott, E.J., and Firestone, F.A., "Specifying Surface Quality", Mechanical Engineering, Vol. 55, 1933, p. 569.
4. Ling, F.F., "On Asperity Distributions of Metallic Surfaces", Journal of Applied Physics, Vol. 29, No. 8, 1958, p. 1168.
5. Thornley, R.H., Connolly, R., Barash, M.M., and Koenigsberger, F., "The Effect of Surface Topography Upon the Static Stiffness of Machine Tool Joints", The International Journal of Machine Tool Design and Research, Vol. 5, 1965, p. 57.
6. Connolly, R., and Thornley, R.H., "Determining the Normal Stiffness of Joint Faces", A.S.M.E. Paper No. 67-Prod.-6, 1967.
7. Ansell, C.T., and Taylor, J., "The Surface Finishing Properties of a Carbide and Ceramic Tool", Proceedings of the Third International Machine Tool Design and Research Conference, University of Birmingham, 1962, p. 225.
8. Archard, J.F., "Contact and Rubbing of Flat Surfaces", Journal of Applied Physics, Vol. 24, No. 8, 1953, p. 981.

APPENDIX A

Geometry of a surface produced by a single point cutting tool

A.1 Assumptions

(1) The surface is smooth before the finish cut.

(2) The final profile follows the circular contour of the tool as shown in Figure A-1.

A.2 Size of the tool marks

If the tip radius and angle of the tool are R and θ, Figure A-2, the maximum depth of cut that will produce the profile in Figure A-1 is:

$$D_{max} = R - R \sin \theta/2$$

For a given depth of cut, $D < D_{max}$, the maximum feed rate that will produce the profile in Figure A-1 is:

$$F_{max} = 2 \sqrt{2DR - D^2}$$

Providing the depth of cut and feed rate are less than these maximum values, the height of the tool marks is:

$$d = R - \sqrt{R^2 - F^2/4}$$

A.3 CLA value

Refer the profile to the coordinates in Figure A-3.

$$y = R - \sqrt{R - x^2}$$

$$\sqrt{R - x^2} \approx R \{1 - \frac{1}{2} (\frac{x}{R})^2\} ,$$

neglecting 4th order and higher power terms

$$y \approx \frac{R}{2} (\frac{x}{R})^2$$

Choose the mean line $\overline{y}$ so that

$$\int_0^{F/2} (y - \overline{y})^2 \, dx \rightarrow \text{minimum}$$

$$\int_0^{F/2} (y - \overline{y}) \, dx = 0$$

$$\therefore \qquad \overline{y} = \frac{R}{6} (\frac{F}{2R})^2$$

at $y = \overline{y}$, $x = \overline{x}$

$$\frac{\overline{x}}{R} = \frac{1}{\sqrt{3}} (\frac{F}{2R})$$

$$\text{CLA} = \frac{2}{F} \int_0^{F/2} |y - \overline{y}| \, dx$$

$$= \frac{2}{F}\ 2 \int_{o}^{\overline{x}} (\overline{y} - y)\ dx$$

$$\therefore \quad CLA = \frac{4R}{F} \int_{o}^{\overline{x}/R} \left[\frac{1}{6} R\left(\frac{F}{2R}\right)^2 - \frac{1}{2} R\left(\frac{x}{R}\right)^2\right]\ d\left(\frac{x}{R}\right)$$

$$CLA = \frac{F^2}{18\sqrt{3}\ R}$$ (formula used by Ansell and Taylor [7])

A.4 Bearing Area

Refer the profile to the coordinates in Figure A-4.

$$y = \sqrt{R^2 - (x + R - d)^2}$$

and

$$d = R - \sqrt{R^2 - F^2/4}$$

$$\therefore \quad y = \sqrt{F^2/4 - 2x\sqrt{R^2 - F^2/4} - x^2}$$

The bearing area, A, is referred to the tip of the tool marks.

$$A = 2/F\ (F/2 - y)$$

$$\therefore \quad y = 1 - 2/F \sqrt{F^2/4 - 2x\sqrt{R^2 - F^2/4} - x^2}$$

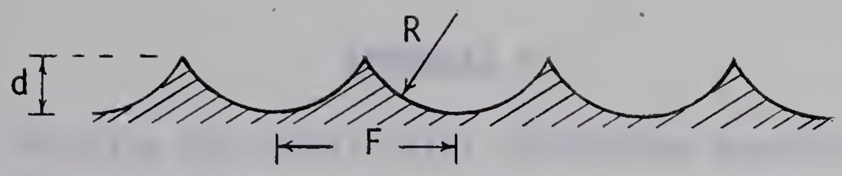

Figure A-1 Surface Profile

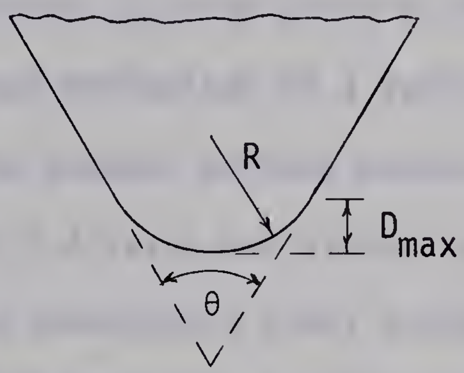

Figure A-2 Cutting Tool

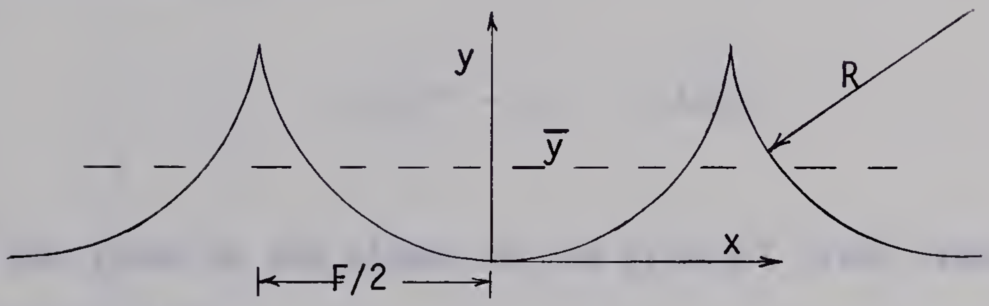

Figure A-3 Coordinates for CLA Value

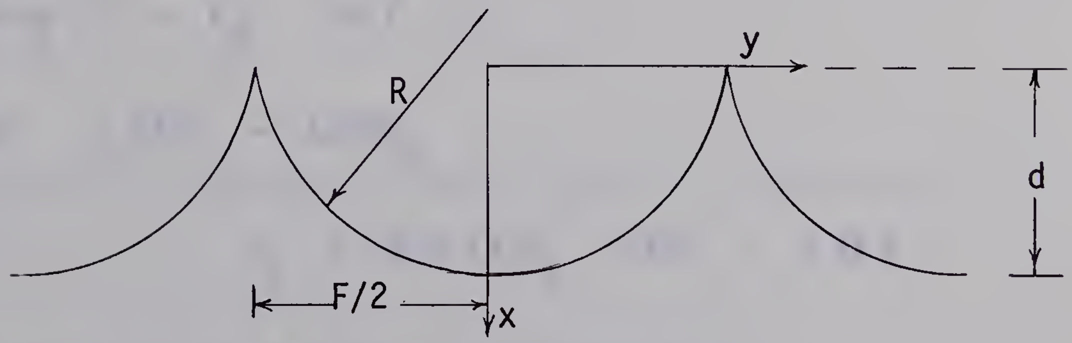

Figure A-4 Coordinates for Bearing Area

[illegible]

[illegible]

[illegible]

[illegible]

APPENDIX B

Relation for total joint deflection reported by Connolly and Thornley [6]

Connolly and Thornley [6] have given an empirical relationship between the initial normal deflection of a joint, λ_L, the CLA value of the joint surfaces, and the nominal surface pressure, P.

For a given P the CLA value was plotted as a function of $\lambda_L(10) - \lambda_L$ for several shaped and turned mild steel joint specimens. The deflection at 10 tons/in.^{2} (22,400 psi), $\lambda_L(10)$, was used as a datum. Straight lines were drawn through the points for each value of P and the following relation was established:

$$\lambda_L(10) - \lambda_L = \text{CLA}/K,$$

where K was taken as the slopes of the straight lines drawn through the experimental points.

The nominal surface pressure, P, was then plotted as a function of K as shown in Figure B-1.

Using $K = K_o$ at $P = 0$

and $\lambda_L(10) = \text{CLA}/K_o$

$$\lambda_L = \text{CLA}\,(1/K_o - 1/K) = z\,\text{CLA}$$

The function, z, is also shown in Figure B-1.

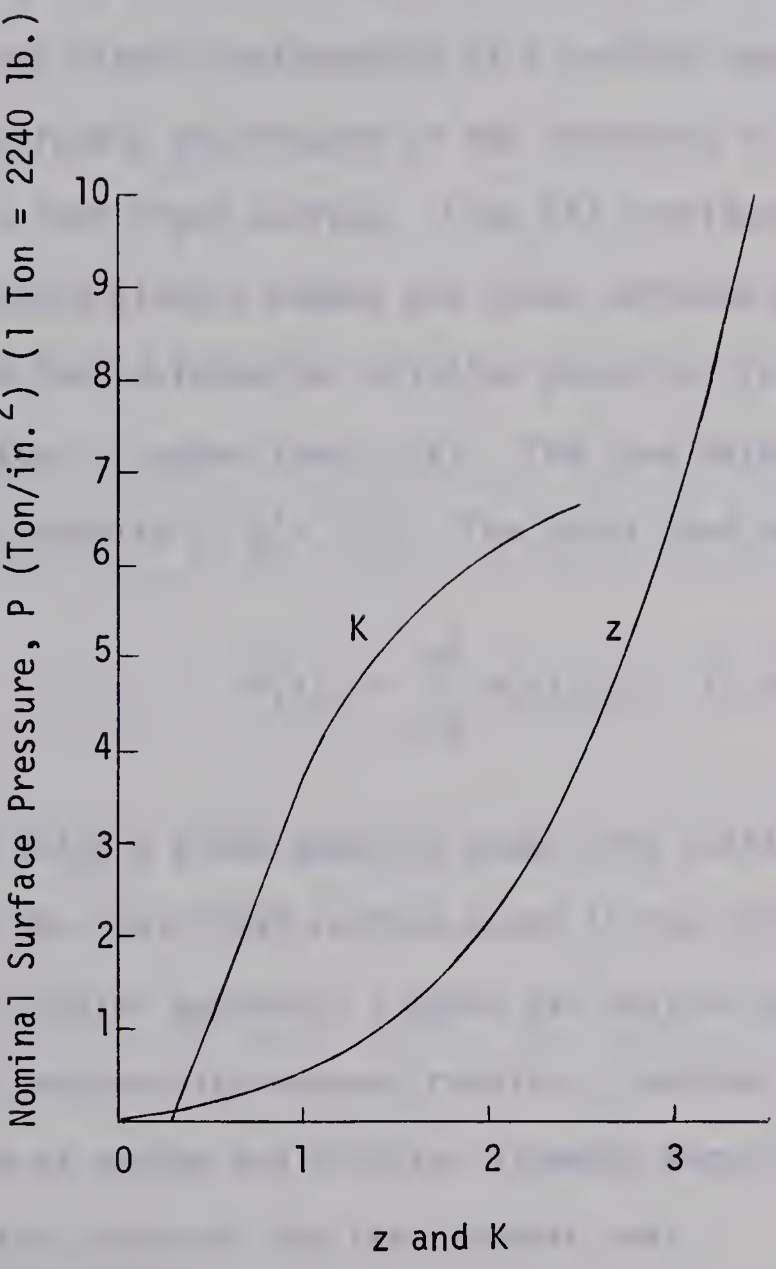

Figure B-1 Functions z and K, Connolly and Thornley [6]

[illegible]

[illegible]

APPENDIX C

Model for surface displacement

Attempts have been made to develop models that represent surface deformation in the direction of the normal load. Archard [8] considered the elastic and plastic deformation of a surface composed of spherical asperities uniformly distributed in the direction of the load and loaded with a flat rigid surface. Ling [4] considered asperities in the form of rigid plastic wedges and cones deformed by a flat rigid surface. The load deformation relation given by Ling assumes a continuous distribution of asperities, $n(\xi)$. The load deformation relation for a single asperity is $p(x - \xi)$. The total load applied to the surface is:

$$P(x) = \int_0^x n(\xi)\, p(x - \xi)\, d\xi$$

The level at which a given asperity comes into contact is ξ and x is the distance the rigid flat surface moves in the direction of the load.

Using a similar approach, a model was devised to qualitatively describe the surface displacement results. Consider one asperity to be a combination of spring and friction elements shown in Figure C-1. The load deflection relations for the elements are:

$p(x) = f(x_1)$ for the elastic spring element

$p(x) = g(x_2)$ for the friction element

x = total distance the load has moved

x_2 = distance the friction element has moved

$x_1 = x - x_2$.

Assume $f(x_1)$ and $g(x_2)$ are continuous and the load deflection relations for the combination of the two elements is as shown in Figure C-2.

Assume a large number of these elements distributed in the direction of the load, $n(\xi)$ elements per unit distance.

$$n(\xi) \quad \text{is continuous} \quad 0 \leq \xi \leq \xi_1 \ ,$$

$$n(\xi) = 0 \ , \quad \xi > \xi_1 \qquad \text{(Figure C-3)}$$

Loading

The load is applied through a flat rigid surface and $P(x)$ is the total load supported by the elements in contact when the load is first applied

$$P(x) = \int_0^x n(\xi)\, p(x - \xi)\, d\xi \ , \qquad \xi \leq \xi_1$$

$$P(x) = \int_0^{\xi_1} n(\xi)\, p(x - \xi)\, d\xi \ , \qquad \xi > \xi_1$$

This corresponds to the total surface displacement curve.

Unloading

Let the total maximum distance through which the load moves be x_m, Figure C-4. Consider an element that initially comes in contact at ξ and is deformed a distance $x_m - \xi$. The maximum load supported by this single element is $p(x_m - \xi)$ and the maximum elastic displacement of this element, $\overline{x}_1$, is defined by:

$$p(x_m - \xi) = f(\bar{x}_1)$$

During unloading, this single element will have an elastic displacement

$$x_1 = x - (x_m - \bar{x}_1) \quad , \qquad \text{(Figure C-4)}$$

A given element will just break contact if it initially comes in contact at $\bar{\xi}$.

$$x_1 = 0$$

$$\bar{x}_1 = x_m - x$$

During unloading and subsequent reloading for $x \leq x_m$:

$$P(x, x_m) = \int_0^{\bar{\xi}} n(\xi)\, f(x - x_m + \bar{x}_1)\, d\xi \qquad \bar{\xi} < \xi_1$$

$$P(x, x_m) = \int_0^{\xi_1} n(\xi)\, f(x - x_m + \bar{x}_1) \qquad \bar{\xi} > \xi_1$$

This corresponds to a recoverable surface displacement curve.

Loading Envelope

The loading envelope for the model, Figure C-5, has characteristics similar to the experimental surface displacement results. The total displacement is part elastic and part plastic. The recoverable displacement curves are the same for loading and unloading, but are affected by the loading history. No attempt was made in this thesis to relate these theoretical curves to those obtained experimentally. This could be the subject of a future research project.

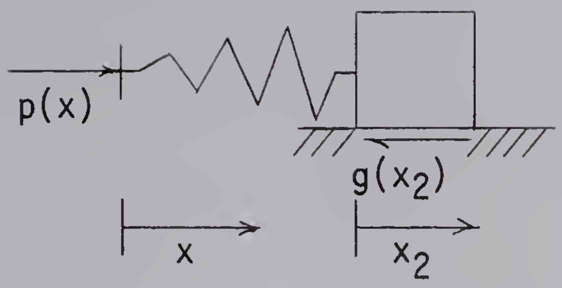

Figure C-1 Combination of Friction and Spring Elements

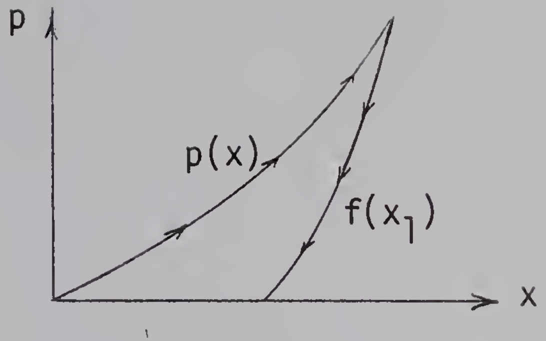

Figure C-2 Load-Deflection Curve for One Set of Elements

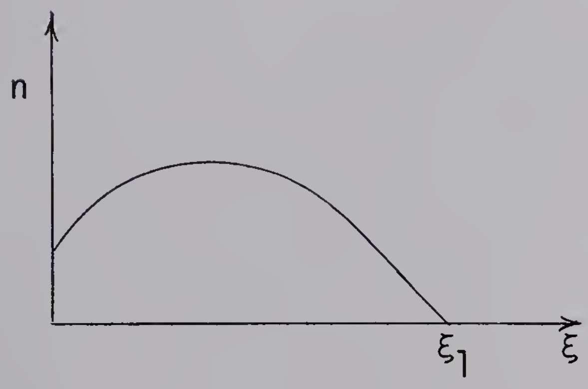

Figure C-3 Distribution of Elements

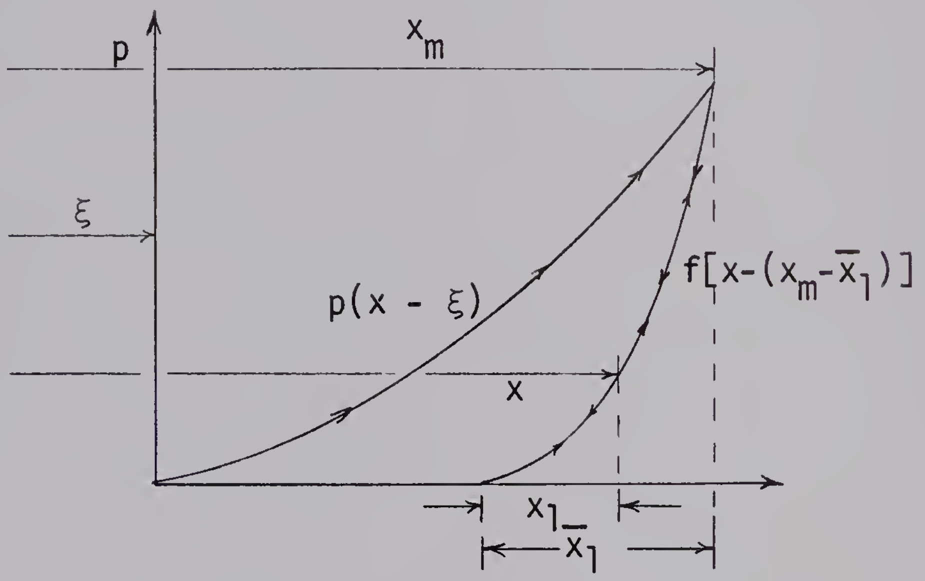

Figure C-4 Deflection of One Element

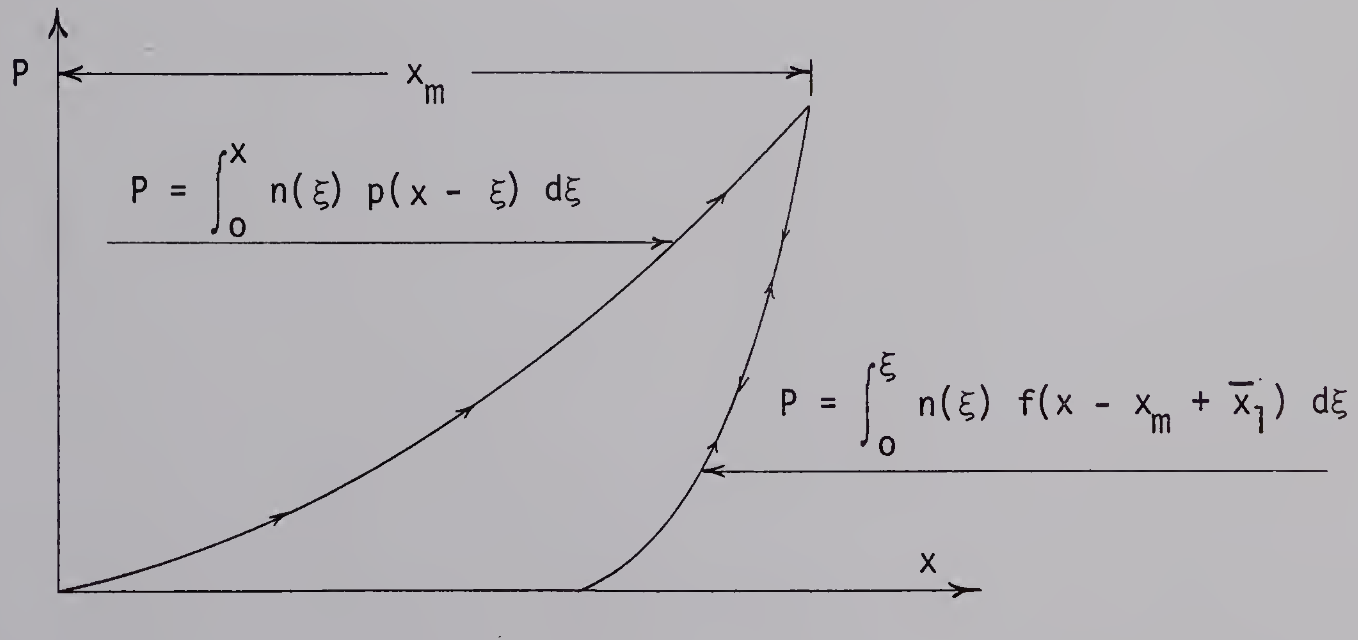

Figure C-5 Loading Envelope